

***Part II***  
***Tensile failures***

# 3

## INTRODUCTION

The easiest way of studying the mechanical properties of fibres is to take a single fibre, grip the two ends to give a defined test length, and then extend it to break on a tensile tester. The measured load and elongation can be converted to provide the axial stress–strain curve of the fibre. The technique is schematically indicated in Fig. 3.1; and Fig. 3.2 illustrates some of the variety of shape of stress–strain curves observed.

For fuller accounts of the mechanical properties, see Morton and Hearle (1993) and Booth (1961). The end–points of these tests are the tensile breaks illustrated in the following chapters. There are many forms of tensile testers, and a number of test parameters which must be specified and controlled in order to obtain valid quantitative data, although these will not usually affect the qualitative forms of break which are described in this book. Generally, the tensile breaks shown here will have been made on a constant–rate–of–elongation Instron tester, with a test length between 1 cm and 10 cm, a rate of extension selected to give a time–to–break between 10 s and 100 s, in an atmospheric environment controlled at 20°C, 65% r.h. Where there are major departures from these conditions, for example in high–speed or wet testing, this will be specially noted.

### A NOTE ON UNITS

*Elongation* is normalized by division by the initial test length to give *strain*, which is then usually multiplied by 100 to give *extension* per cent.

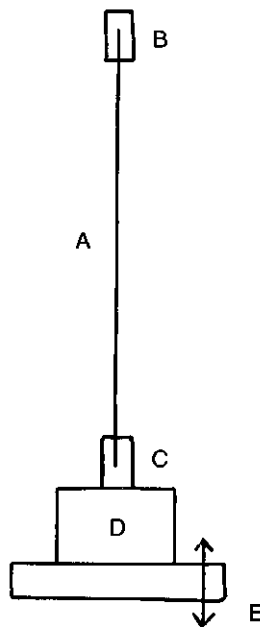


Fig. 3.1— Typical arrangement of tensile tester: (A) fibre specimen; (B) upper jaws; (C) lower jaws; (D) load-cell; (E) cross-head.

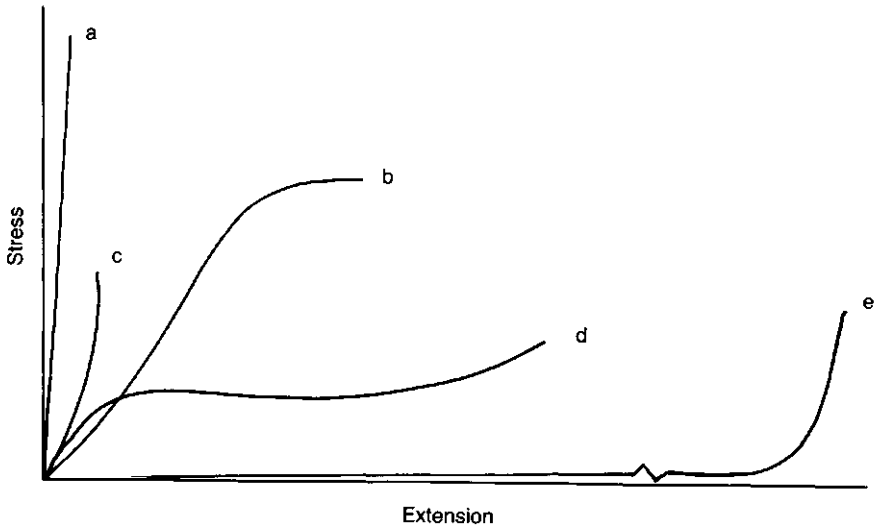


Fig. 3.2 — Typical stress–strain curves of fibres: (a) strong inextensible fibre; (b) tough synthetic fibre; (c) cotton and other plant fibres; (d) weak man-made fibre; (e) elastomeric fibre.

*Load* (force, tension) may be divided by area of cross-section to give *stress*, but in fibre technology is more commonly and usefully divided by linear density, namely mass per unit length, to give *specific stress*.

Unfortunately, there is a great diversity of units for both stress and specific stress, and an equivalence of quantities, such as energy/mass or stress/density for specific stress. A full conversion chart is given by Hearle (1982). A few examples are:

linear density: 1 tex = 1 g/km  
 1 denier = 1 g per 9000 m  
 specific stress: 1 N/tex = 1 kJ/g = 1 GPa/(gcm<sup>3</sup>)  
 1 gf/tex = 9.8 mN/tex  
 1 gf/den = 0.0885 N/tex

# 4

## BRITTLE TENSILE FRACTURE

### Glass, ceramic, carbon, elastomeric fibres

Inorganic fibres such as glass have a simple Hookean stress-strain curve, line (a) in Fig. 3.2, and the sharp break is reflected in the clean failure, which may appear as a single flat cleavage plane perpendicular to the fibre axis, 4A(1). More commonly, the very smooth region is limited to an approximately semicircular zone centred on the start of crack propagation, and the remainder of the break, while still perpendicular to the fibre axis, has a rougher, hackled appearance, 4A(2)–(4).

This form of break is the classical brittle fracture, which obeys the linear elastic fracture mechanics first introduced by Griffith. The surface of the fibre inevitably contains a number of cracks or flaws, as indicated in Fig. 4.1(a). When tension is applied, there is a stress concentration at the tip of each crack, which increases in magnitude with crack depth. As the load on the fibre increases, the largest stress concentration at the deepest flaw eventually exceeds the local tensile strength of the material, which ruptures and so causes the crack to start to grow, Fig. 4.1(b). Since the stress concentration then increases, the growth continues catastrophically to give the smooth 'mirror' region extending radially outwards from the initial flaw, Fig. 4.1(c). This continues until the stress on the part of the fibre ahead of the crack reaches a level at which further crack growth starts from internal flaws to give the rougher region, Fig. 4.1(d). The broken fibre shows the mirror region A and the hackled region B, Fig. 4.1(e).

The fibre strength, which ranges from about 0.75 N/tex (1.9 GPa) up to 1.8 N/tex (4.5 GPa) in the strongest modern glass fibres, depends partly on the inherent structure but is also

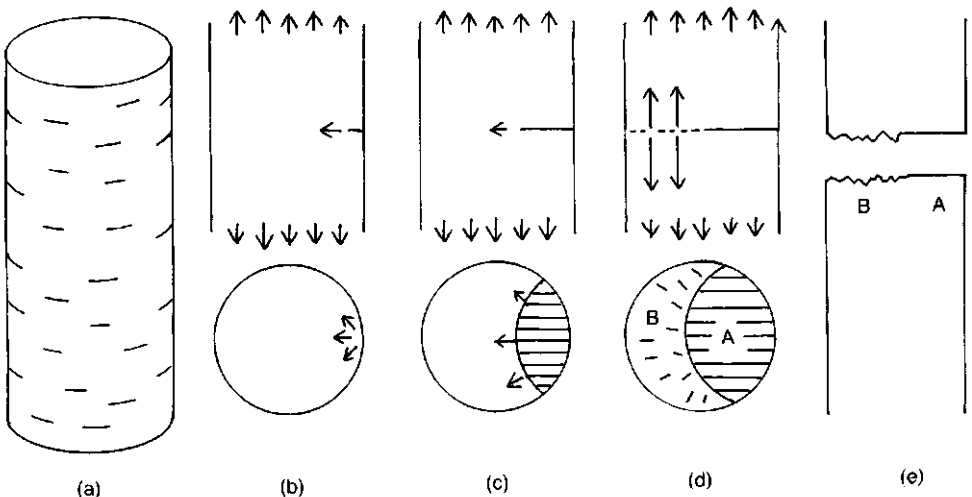


Fig. 4.1 — (a) Glass fibre, indicating surface flaws. (b) When tension reaches a given level, the deepest crack starts to propagate. (c) The crack growth continues catastrophically. (d) Eventually the high stress on the unbroken part starts multiple crack growth. (e) The final failure shows a mirror region A and a hackled region B.

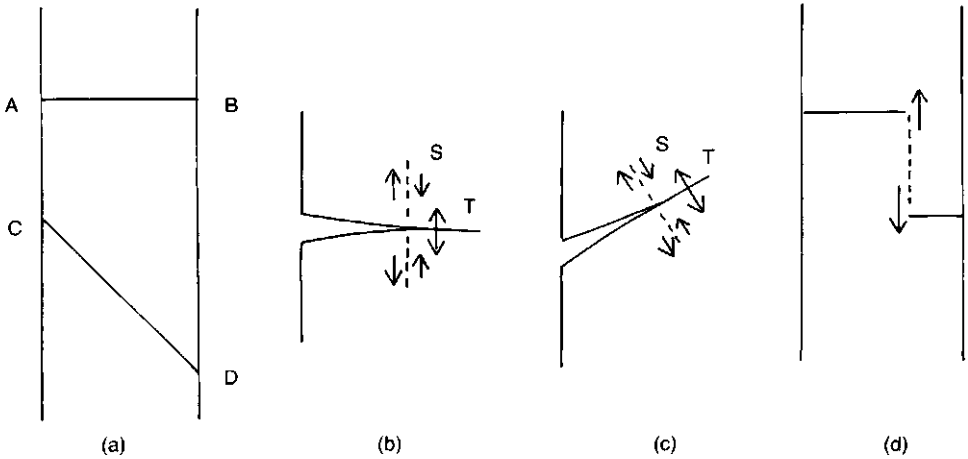


Fig. 4.2— (a) Plane of maximum tensile stress AB, and maximum shear stress CD. (b) Tensile (T) and shear (S) stresses near a crack tip. (c) Tensile (T) and shear (S) stresses when crack is angled. (d) Two separate cracks linked by a plane of high shear stress.

critically dependent on the state of the fibre surface, with the strength decreasing as damage leads to deeper surface cracks. Glass fibres show greater strength than bulk glass, which commonly contains surface cracks much larger than the few micrometres of a fibre diameter.

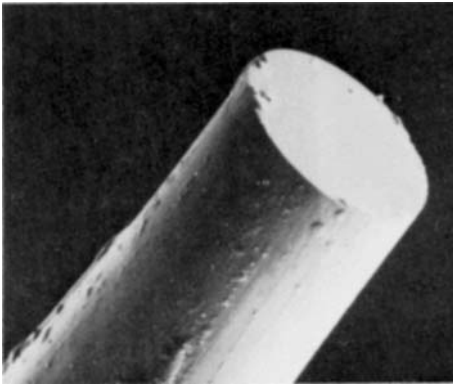
An essential feature of the pure form of brittle fracture is that the material strain is everywhere elastic, with no plastic yield. As an alternative to the formulation in terms of stress concentration and material strength, the fracture mechanics may be expressed by the criterion that crack growth will occur when the reduction in elastic strain energy, due to unloading of material near the growing crack, exceeds the surface energy of the newly exposed material (see Chapter 1).

Although breaks perpendicular to the fibre axis are the simplest form and are frequently observed, it is not uncommon to find cracks at other angles, **4A(5),(6)**. There are a number of possible reasons for the changes of direction. The line of maximum tensile stress in the whole fibre is across a plane perpendicular to the fibre axis, and locally it is along the line of crack opening: these two directions usually coincide to give the fractures perpendicularly across the fibre. However, there is also a line of maximum shear stress in the whole fibre at  $45^\circ$  to the fibre axis, and locally there is shear stress perpendicular to the crack. These stresses are indicated in Fig. 4.2(a)–(c) and it is obvious that they could turn the crack into other directions of propagation. Another possibility is that two separate cracks develop, and that these then become linked by shear failure between them, Fig. 4.2(d).

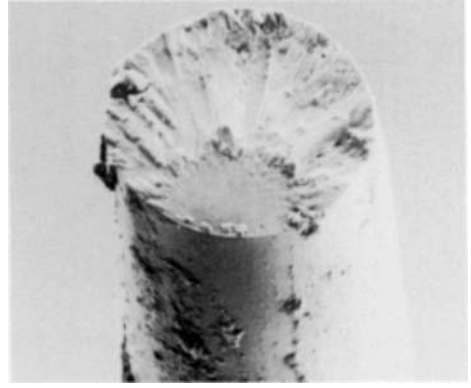
Brittle fracture is also shown by other inorganic fibres, **4B(1)–(6)**: these are ceramic fibres with high-modulus linear stress–strain curves, type (a) in Fig. 3.2. The fibre strengths may be comparatively low in fibres intended for uses such as thermal insulation, but will be high in reinforcing fibres. The breaking extension is always very low. Most of these ceramic fibre breaks are very similar to those of glass fibres, but the ICI Saffil (alumina) fracture surface does show appreciable granulation. In other alumina fibres (see Chapter 8), the granulation is much more pronounced, so that the breaks are regarded as falling in a different category.

Another high-modulus fibre, with a stress–strain curve of type (a) in Fig. 3.2, and a smooth fibre brittle failure, is carbon fibre, **4C(1)–(3)**, although this form is shown only by certain types of carbon fibre, notably those with a viscose rayon precursor. Other carbon fibres show granular breaks (see Chapter 8).

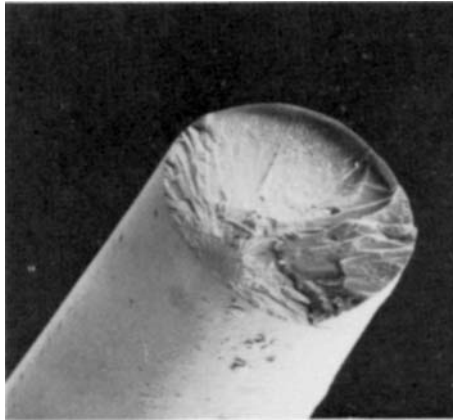
More surprisingly, brittle failure is also found in fibres at the opposite end of the spectrum: the low-modulus, highly extensible elastomeric fibres, **4C(4)–(6)**, with stress–strain curves of type (e) in Fig. 3.2. However, the important point is that the deformation is elastic, and, indeed just before breakage it is also linear and of relatively high modulus. The material is not influenced by the way in which it reached the state near to failure.



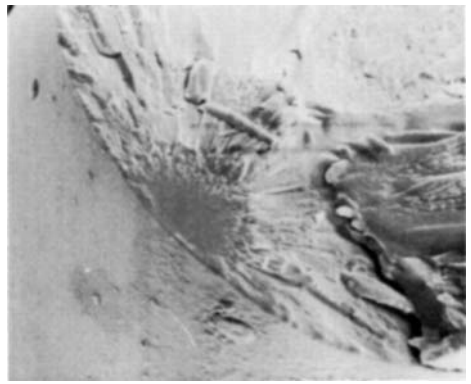
1

 10  $\mu\text{m}$ 


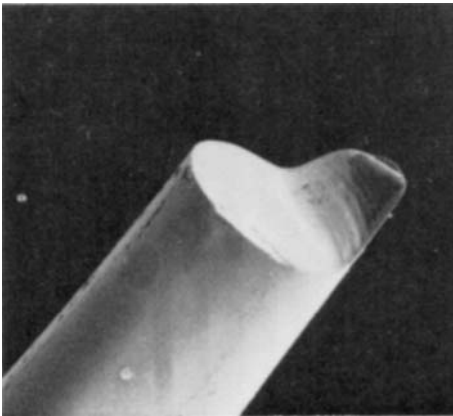
2

 10  $\mu\text{m}$ 


3

 5  $\mu\text{m}$ 


4

 2  $\mu\text{m}$ 


5

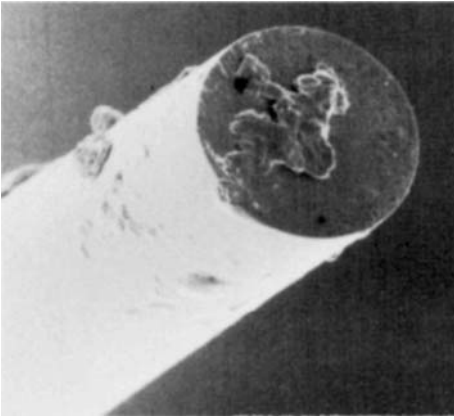
 10  $\mu\text{m}$ 


6

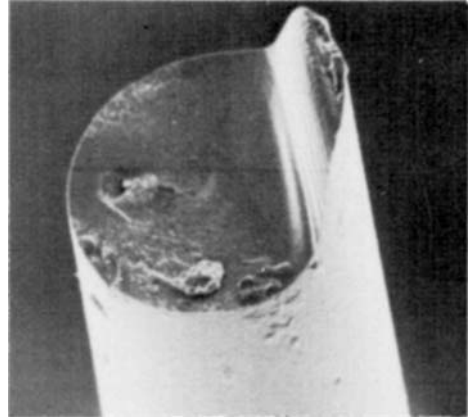
 5  $\mu\text{m}$ 

**Plate 4A — Tensile breaks of glass fibres.**

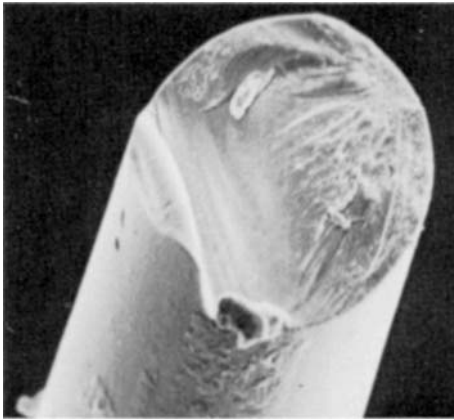
(1) Single cleavage plane. (2) Fracture starting from front, showing mirror and hackled zones. (3) Fracture with smaller mirror zone. (4) Detail of crack initiation, mirror zone and change to hackled zone. (5) Angular displacement at edge of fibre. (6) Crack propagation with failure in a plane not perpendicular to fibre axis.



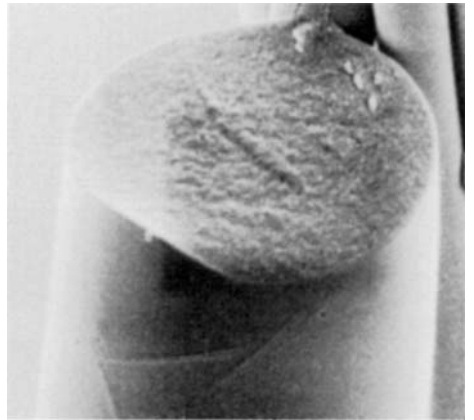
1

5  $\mu\text{m}$ 

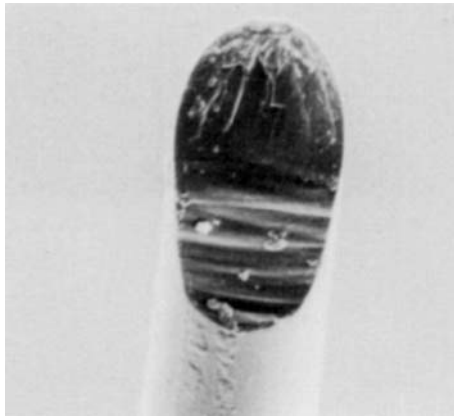
2

2  $\mu\text{m}$ 

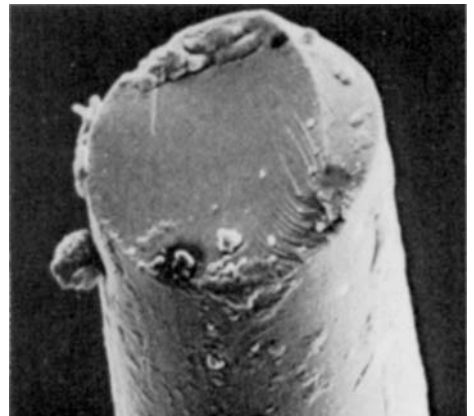
3

5  $\mu\text{m}$ 

4

5  $\mu\text{m}$ 

5

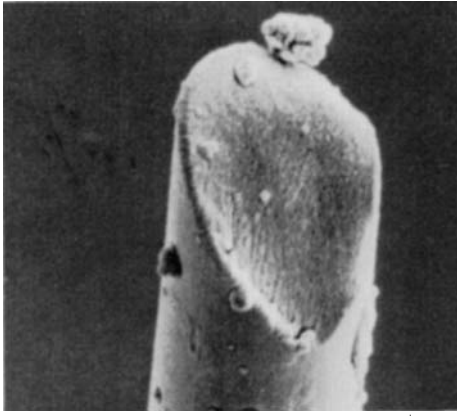
10  $\mu\text{m}$ 

6

5  $\mu\text{m}$ 

**Plate 4B — Tensile breaks of ceramic fibres.**

(1) 3M fibre Nextel 312: single cleavage plane with some complication. (2) 3M fibre Nextel 312: crack turning and running along fibre. (3) Sumitomo alumina fibre: crack initiation at top right, leading to angled crack. (4) ICI Saffil alumina fibre: perpendicular crack with slight granulation. (5) Nicolon SiC fibre, NLM 202: angled crack. (6) Nicolon SiC fibre, NLM 202: mixed crack.



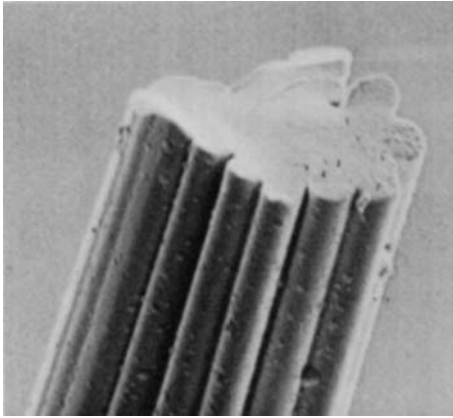
1

5 μm



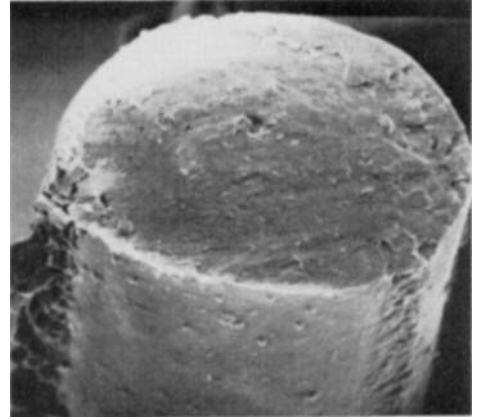
2

2 μm



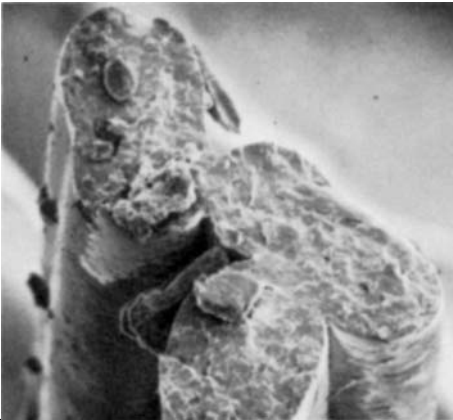
3

5 μm



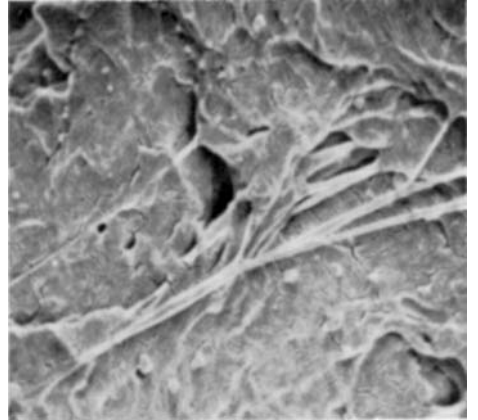
4

5 μm



5

10 μm



6

2 μm

**Plate 4C — Tensile breaks of carbon fibres.**

(1) Hercules fibre AS46K: angled crack. (2) Hercules fibre AS46K: more complicated break. (3) SCL (viscose rayon precursor) fibre: perpendicular fracture.

**Tensile breaks of elastomeric fibres.**

(4) Du Pont Lycra (segmented polyurethane): flat fracture plane. (5) Lycra: break propagated across three fibres which are fused together. (6) Lycra: detail of fracture surface.

# 5

## DUCTILE TENSILE FRACTURE Nylon, polyester, polypropylene, etc.

Rupture of the melt-spun synthetic fibres like nylon is dominated by yield. The tensile strength is essentially the yield stress, as shown by the end of line (b) in Fig. 3.2. This final flat portion of the stress-strain curve is really the end of the long draw which can be applied to an unoriented fibre formed on cooling a filament from the melt.

Study of a thick undrawn nylon monofilament shows up clearly the mechanism of ductile crack propagation leading to break. The load-elongation curve is shown in Fig. 5.1, although because this is a thick, short specimen (10 mm long, 1 mm diameter) the strain values may be falsely exaggerated: break usually occurs in undrawn nylon fibres at extensions of around 500–600%. In the nylon bristle, there is an initial elastic extension until yield occurs; the stress then drops after a small overshoot, and the fibre draws at a neck under a constant stress. With further elongation the neck propagates out of the specimen, and then uniform plastic elongation occurs under a steadily increasing tension. Long before the fibre breaks, a skilled operative can detect where break will occur, and subsequently a large crack is easily visible.

The form of break is shown in 5A(1), and the way it develops in 5A(2). Three main regions can be identified in the break, as illustrated in Fig. 5.2: initiation at A, stable crack propagation at B, and final catastrophic failure at C. These zones are also present in the breaks of finer fibres, but there are some special features to be noted in the thick monofilament. The initiation, shown in 5A(3),(4), is due to a development of voids below the fibre surface: these grow and finally coalesce into the crack. The surface of the crack is concave and has a texture of fine voids. It thus appears that cavitation, rather like crazing in glassy plastics, is the detailed way in which a crack forms. The transition from the crack B to the final failure zone C shows a structure of ridges, seen in 5A(5), presumably due to an alternation of break and stick. Finally, the far edge of the catastrophic region shows some irregular tearing. An end-on view of the break, 5A(6), shows how yielding of the unbroken material leads to a great thinning of the cross-section.

Essentially the same type of break is shown by typical nylon textile fibres, 5B(1)–(4), except for some differences in the initiation and transition regions; and studies on films, by Buckley

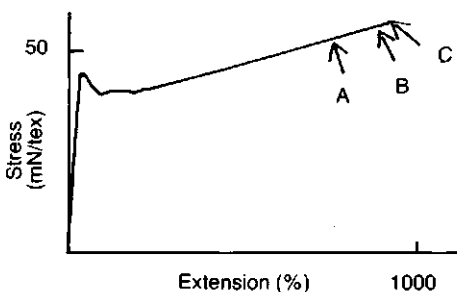


Fig. 5.1 — Load-elongation curve of an undrawn monofilament: crack observed at A; half-way across fibre at B; break at C.

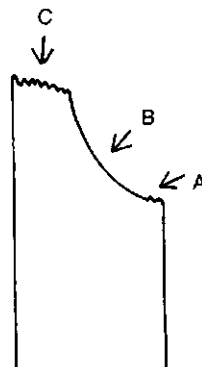


Fig. 5.2 — Ductile break, showing separate regions.

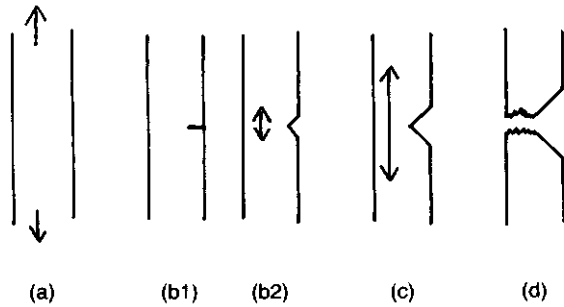


Fig. 5.3 — Sequence of stages in the occurrence of a ductile break. (a) Fibre under load. (b) Crack starts (b1), but immediately opens up (b2). (c) Further crack growth and opening, due to high-yielding extension of the unbroken part. (d) After catastrophic failure.

(1979), **5B(5),(6)**, demonstrate clearly the form of deformation associated with the crack propagation. The mechanisms involved are illustrated schematically in Fig. 5.3. The specimen initially extends uniformly under load, Fig. 5.3(a); but when the tensile stress reaches a certain level, Fig. 5.3 (b1), a crack starts to propagate into the specimen, from a surface flaw on a fibre, from a cut deliberately put in the film, or from self-induced voids in the bristle. Plastic yield (drawing) of material causes the crack to open into a V-notch, Fig. 5.3(b2), which propagates steadily into the specimen, Fig. 5.3(c). The discontinuous separation at the open end of the V is linked to the continuous elongation on the other side by the long zone of plastic shear shown in **5B(5)**. Finally catastrophic failure occurs under the high stress on the unbroken part of the cross-section, Fig. 5.3(d). Similar forms of failure have been reported in plastic films by Walker, Haward and Hay (1979). The fracture mechanics is very complicated in stress and strain distribution and has not been analysed. Distortion of the break occurs when the film specimen is cut at an angle to the orientation direction, **5B(6)**: this picture also shows thinning of the film due to the high plastic extension on the opposite side to the crack.

Although the ductile V-notch break is the common form, there are several variants in the form of nylon breaks. Increasing the rate of strain, without going to ballistic impact and the change of mechanism described in Chapter 6, causes the size of the crack region to decrease relative to the final failure region, with changes from over 50% in **5B(3)**, to 40% and less than 20% in **5B(1)** and **(4)**, respectively.

Initiation may be at a crack or flaw perpendicular to the fibre axis, as in **5B(1)**, or at a point, **5C(1)**, or points, a wide line, **5C(2)**, or an angled line, **5C(3)**. The latter distorts the form of the V-notch, and may in extreme cases, such as **5C(4)**, give a multiple final failure zone. Occasionally, cracks develop in two places on the fibre, either opposite one another, **5C(5)**, or axially displaced, **5C(6)**.

In rare circumstances, the break starts internally and not on the surface, as shown in **5D(1)**. This would occur when there is a substantial flaw inside the fibre. The three-dimensional geometry of ductile crack propagation then causes the formation of a double cone within the fibre, leading to the catastrophic failure region. Intermediate forms are shown in **5D(2),(3)**, which are nylon fibres partially oxidized by hydrogen peroxide.

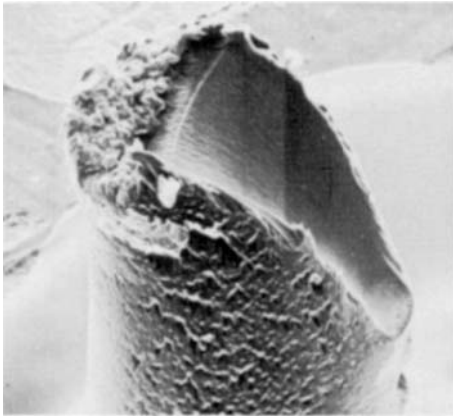
Fibres with a special shape, such as the trilobal nylon in **5D(4)**, show a modified geometry of crack formation.

Although this chapter is concerned with tensile failure, it is worth noting that when a nylon fibre is twisted to break it can show a fracture morphology, similar to tensile breaks, except for a skewing round of the crack, as shown in **5D(5)**. Of more direct relevance is the fact that the tensile failure of a fibre which has been heat set in a twisted state also has a distorted shape. The crack appears to propagate perpendicular to the helical line of the twist, which corresponds to the molecular orientation, as seen in **5D(6)**. There is also some splitting between the lines of orientation, due to shear forces.

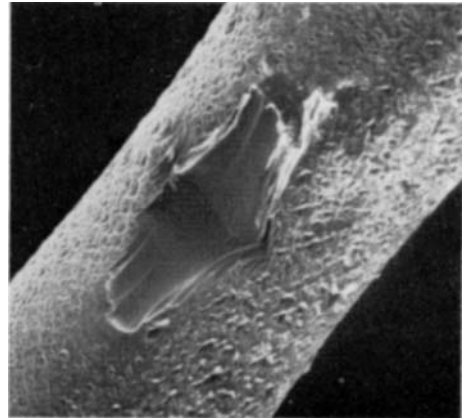
Most of the pictures in **5A–5D** are of nylon 66, but other melt-spun synthetic fibres show similar forms of break: polyester (polyethylene terephthalate) in **5E(1)–(3)** and nylon 6 in **5E(4)**. Polypropylene also shows a V-notch leading to a catastrophic region, **5E(5)**, but due to features of chemical and physical structure, which affect its melting and thermomechanical behaviour, always shows a more disturbed final failure region, with pieces of material sticking out from the break. Sometimes the V-notch is almost lost in the confusion **5E(6)**.

In most tensile tests of normal nylon and polyester fibres, with a typical test length, say 5 cm, the failure will usually develop through a crack from one point on the fibre surface. Occasionally, there may be two cracks, and sometimes they are internal. However, in some fibres, where the surface must have been affected in an unusual way, a line of separate cracks appears, with one happening to propagate first to rupture: examples are shown in **5F(1),(2)**.

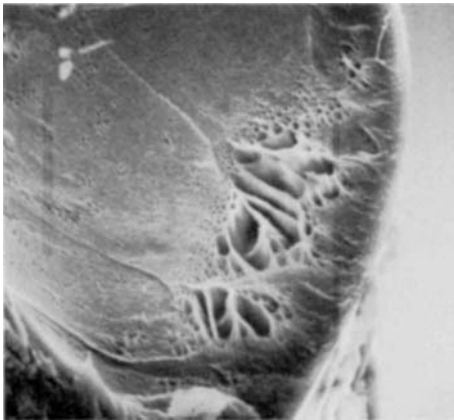
Studies of crack development on a polyester monofilament confirm that the cracks start to develop and grow shortly before the final rupture occurs. Cracks as they exist at 38% and 40% extension are shown in **5F(3),(4)**, for a fibre which breaks at a little more than 40% extension with the form shown in **5E(1)**.



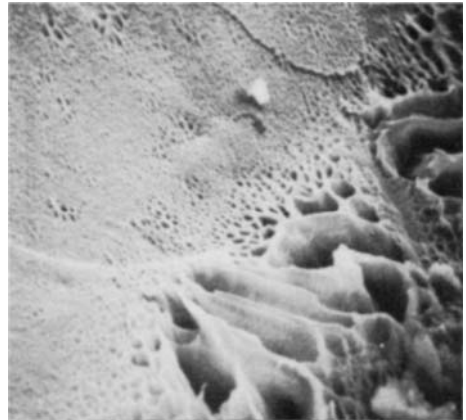
1

 100  $\mu\text{m}$ 


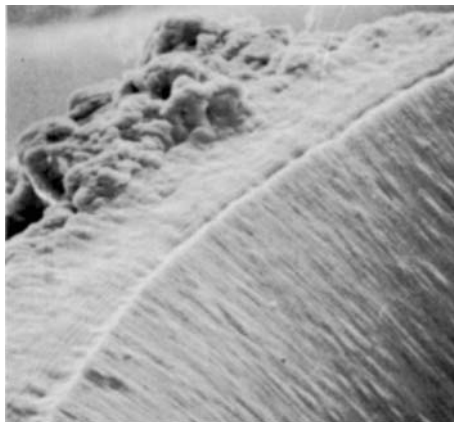
2

 100  $\mu\text{m}$ 


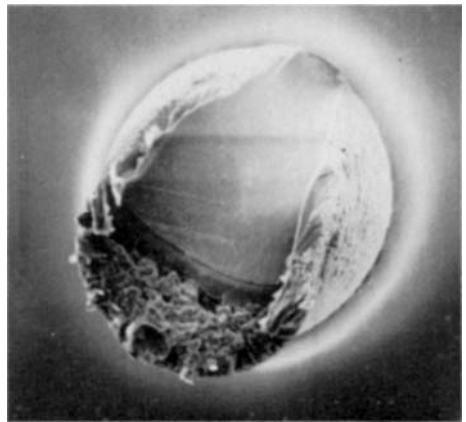
3

 10  $\mu\text{m}$ 


4

 5  $\mu\text{m}$ 


5

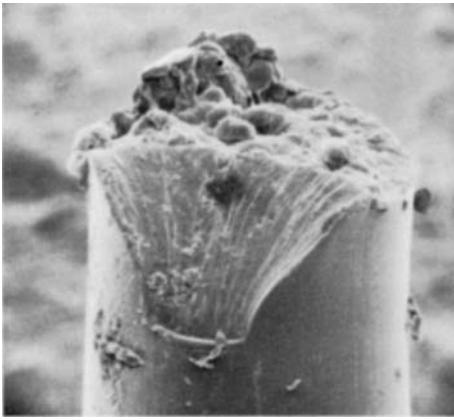
 20  $\mu\text{m}$ 


6

 100  $\mu\text{m}$ 

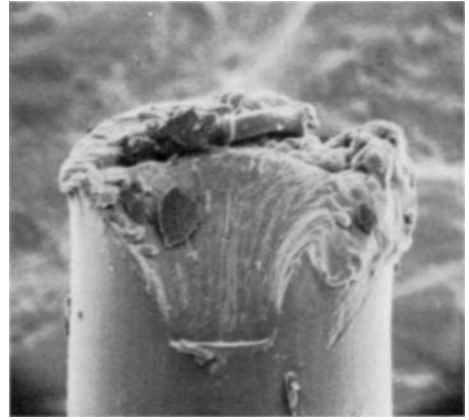
**Plate 5A — Rupture of a coarse undrawn nylon 66 bristle, 1 mm diameter, extended at a strain rate of  $8 \times 10^{-4} \text{ s}^{-1}$  (see Fig. 5.1).**

(1) Broken end, showing initiation at bottom right (A in Fig. 5.2), ductile crack growth across fibre (B), and final failure at top left (C). (2) Propagating crack, from fibre removed from test before break. (3) Initiation region, showing start of crack at large voids. (4) Detail showing transition from large voids in initiation to small voids in growth region. (5) Transition from region of stable crack growth to final catastrophic failure region. Note also irregular tearing at far edge of crack. (6) End-on view of broken fibre. Note thinning of cross-section due to local drawing of material near break.



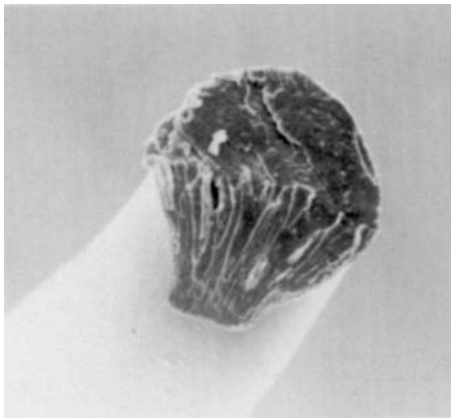
1

|——| 10 μm



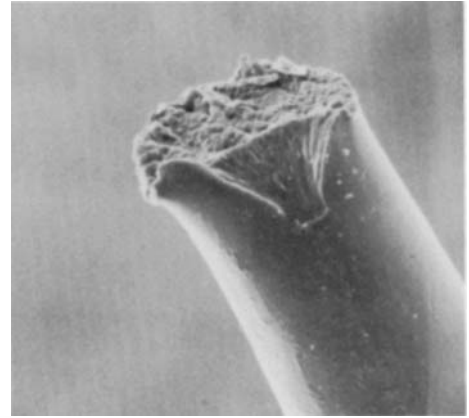
2

|——| 10 μm



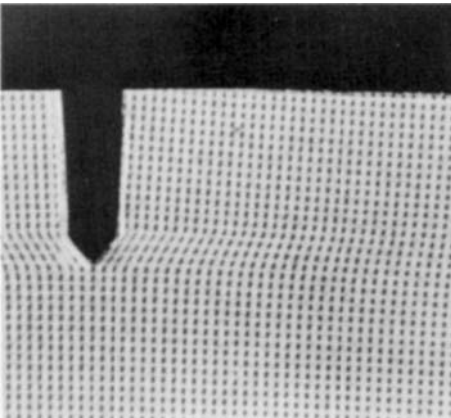
3

|——| 10 μm

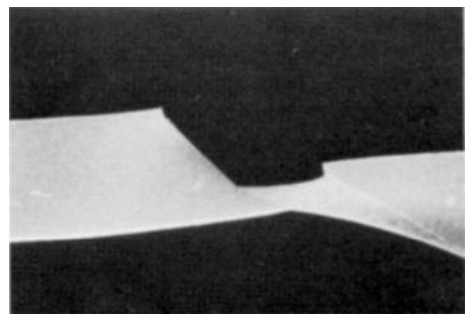


4

|——| 10 μm



5



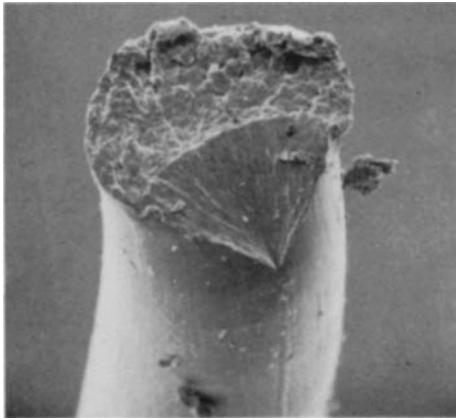
6

**Plate 5B — Tensile break of nylon fibres.**

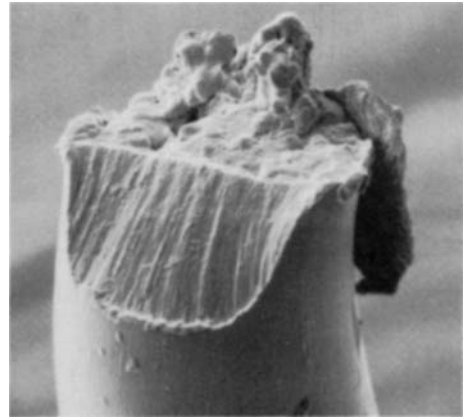
(1) 17 dtex nylon 66 fibre, broken by extension at strain rate of  $1.67 \times 10^{-2} \text{ s}^{-1}$ . Failure starts from a line perpendicular to the fibre axis. Ductile crack crosses about 40% of fibre thickness before catastrophic failure. (2) Opposite end of same nylon 66 break. (3) Nylon fibre, as (1), broken at low rate of strain,  $1.67 \times 10^{-4} \text{ s}^{-1}$ , with ductile crack covering 50% of fibre. (4) Nylon fibre, as (1), broken at higher rate of strain,  $3.33 \times 10^{-1} \text{ s}^{-1}$ , with crack penetrating less than 20% of thickness.

**Tensile break of polyester film.**

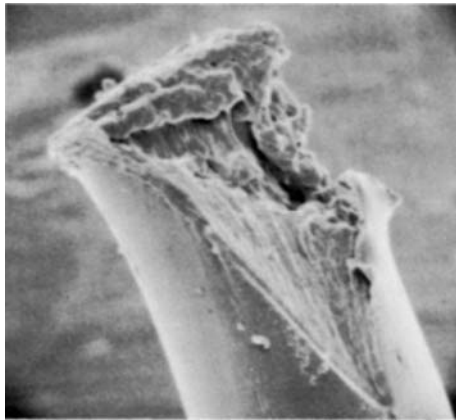
(5) Polyester (PET) film, with crack growth from an initial cut. Grid shows strain distribution. (6) Polyester film extended at an angle to orientation direction, showing distortion of crack growth and yield.



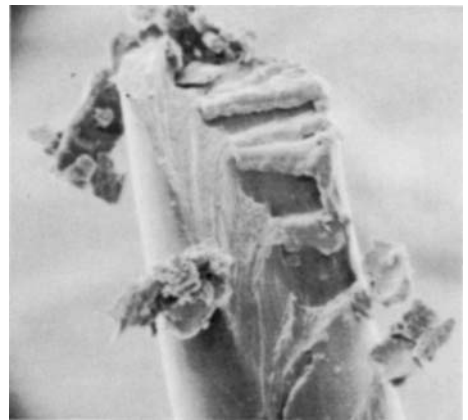
1

 10  $\mu\text{m}$ 


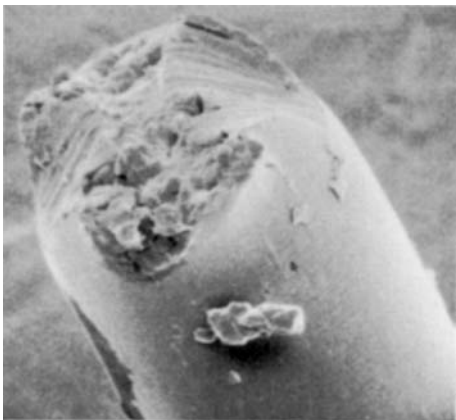
2

 10  $\mu\text{m}$ 


3

 5  $\mu\text{m}$ 


4

 5  $\mu\text{m}$ 


5

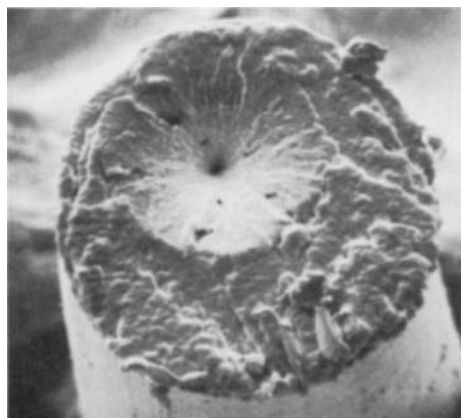
 10  $\mu\text{m}$ 


6

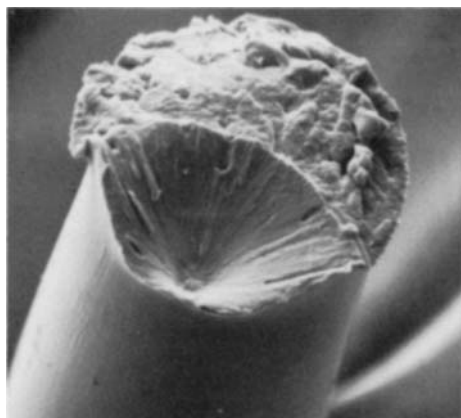
 10  $\mu\text{m}$ 

**Plate 5C — Tensile breaks of nylon fibres.**

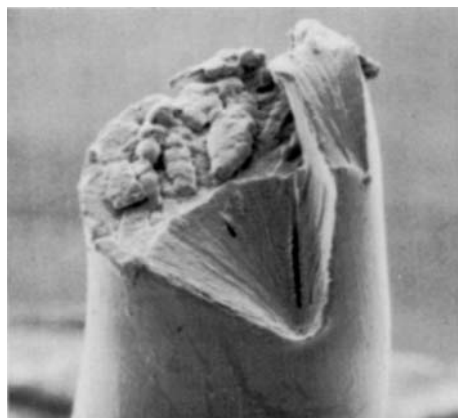
(1) Experimental nylon 66 filament, with initiation of break at a point. (2) Break of nylon 66 fibre, previously immersed in 30 vol.  $\text{H}_2\text{O}_2$  for 2 hours, with wide initiation zone. (3) 4.5 dtex nylon 66 fibre, with break initiated at an angled linear flaw. (4) 4.5 dtex nylon 66 fibre, with inclined initiation leading to multiple catastrophic failure zones. (5) Ductile crack growth, from initiation at two zones at same axial position in 17 dtex nylon 66. (6) Double crack in 17 dtex nylon 66, starting at two different positions along the fibre, with catastrophic failure propagating axially between the two cracks.



1

 5  $\mu\text{m}$ 


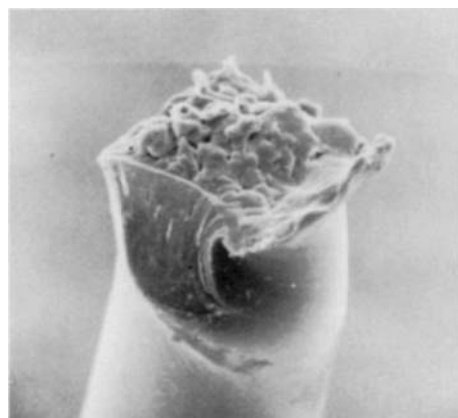
2

 10  $\mu\text{m}$ 


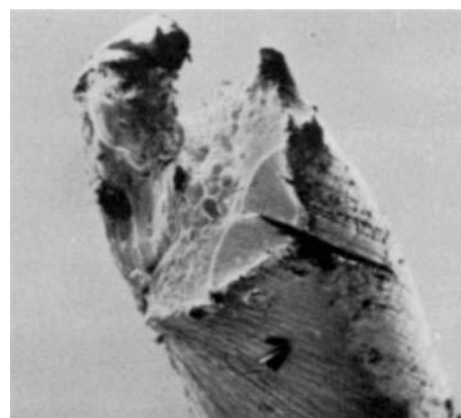
3

 10  $\mu\text{m}$ 


4

 10  $\mu\text{m}$ 


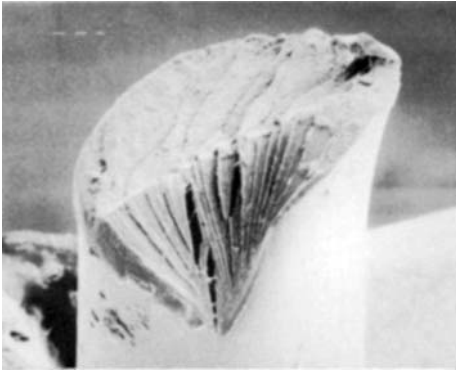
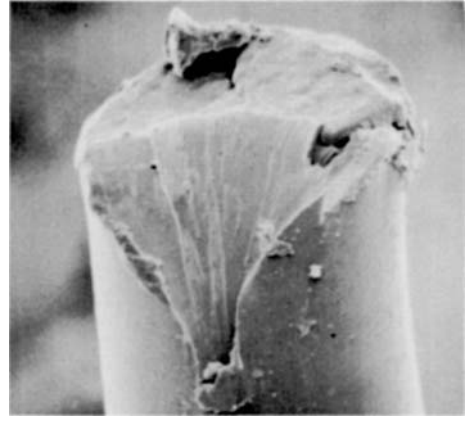
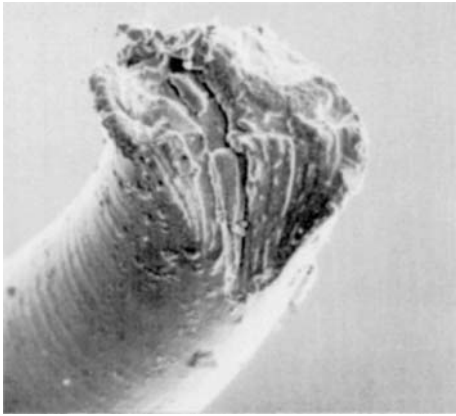
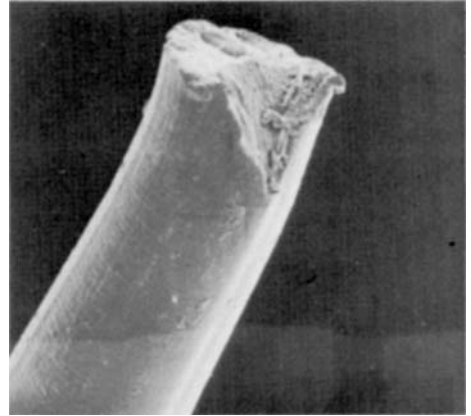
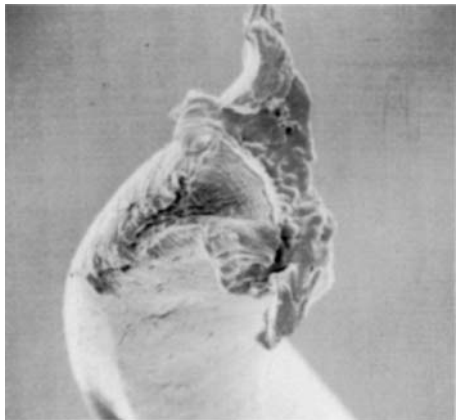
5

 10  $\mu\text{m}$ 


6

**Plate 5D — Tensile breaks of nylon fibres.**

(1) Break starting at an internal fault in 4 dtex nylon 66 fibre, to give a cone-shaped ductile crack zone, surrounded by the catastrophic failure region. (2) Break starting near the edge of a nylon 66 fibre, immersed in 100 vol.  $\text{H}_2\text{O}_2$  for 2 hours, before testing, with a cone developing into a V-notch. (3) A combination of complications in break of nylon 66 fibre, immersed in 30 vol.  $\text{H}_2\text{O}_2$  for 2 hours, including double initiation, internal and external. (4) Rupture of trilobal nylon 66 fibre, with double initiation on separate lobes. (5) 17 dtex nylon 66 fibre twisted to break at 78 turns/cm under constant tension (see also Chapter 24). (6) Tensile fracture of nylon 6 fibre heat set with a surface helix angle of  $34^\circ$ .

1 |-----| 100  $\mu\text{m}$ 2 |-----| 10  $\mu\text{m}$ 3 |-----| 5  $\mu\text{m}$ 4 |-----| 5  $\mu\text{m}$ 5 |-----| 10  $\mu\text{m}$ 6 |-----| 10  $\mu\text{m}$ 

**Plate 5E — Tensile breaks of polyester fibres.**

(1) Break of a thick (0.55 mm diameter) polyester monofilament. (2) Break of a fine polyester fibre, produced on laboratory melt-spinning equipment and drawn 1.5 $\times$ . (3) Break of a commercial polyester fibre.

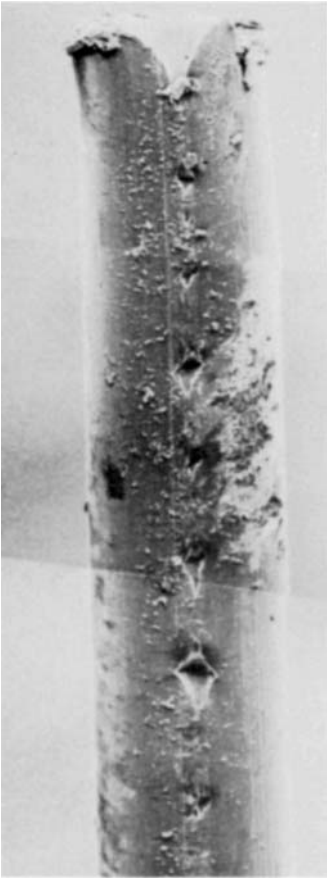
**Tensile break of nylon fibre.**

(4) Break of a nylon 6 fibre.

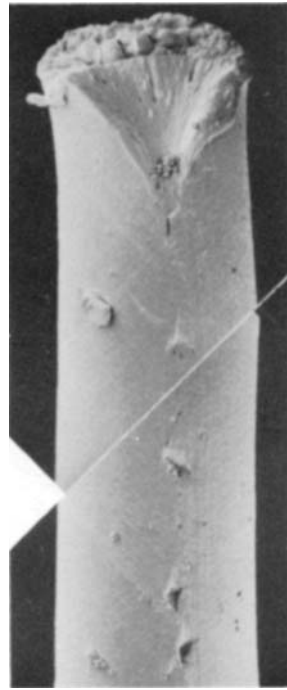
**Tensile break of polypropylene fibre.**

(5) Break of Phillips polypropylene, 8.3 dtex, tenacity of 523 mN/tex, breaking extension of 53%.

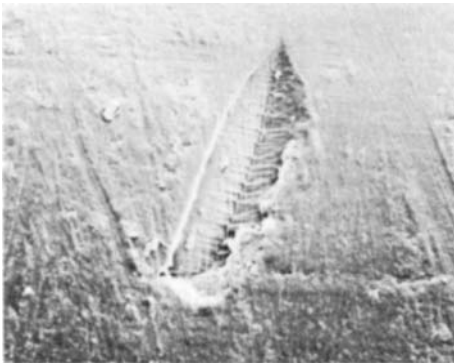
(6) Break of 15.7 dtex AKZO polypropylene fibre.



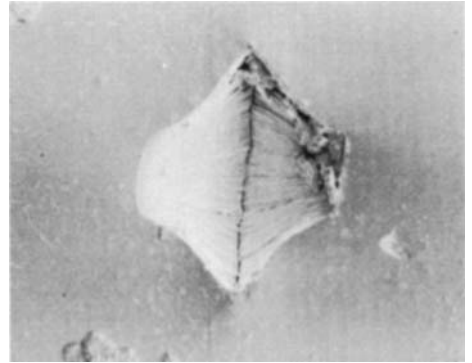
1



2

10  $\mu\text{m}$ 

3

10  $\mu\text{m}$ 

4

10  $\mu\text{m}$ 

**Plate 5F — Tensile breaks of nylon: multiple cracks.**

(1) Nylon 6 fibre from yarn, heat set at 195°C, showing multiple initiation of cracks. (2) Multiple initiation in a commercial nylon 6 fibre with break and partial cracks.

**Tensile test of polyester monofilament (0.5 mm diameter) with final break at just over 40% extension crack development.**

(3) At 38% strain. (4) At 40% strain.

# 6

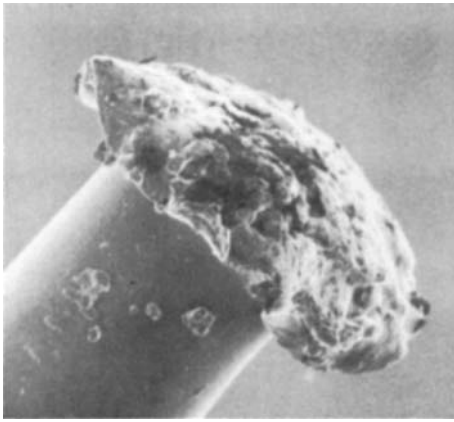
## HIGH-SPEED TENSILE BREAK

### Nylon, polyester and other melt-spun fibres

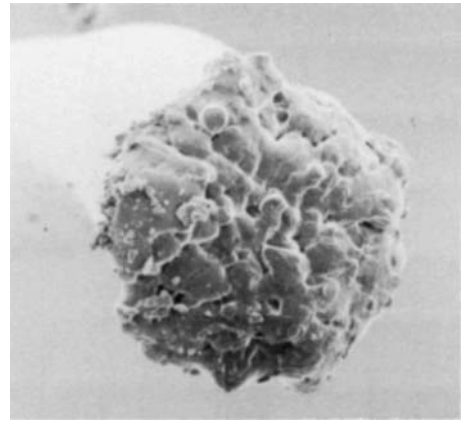
It was noted in Chapter 5 that when the rate of extension was increased the size of the V-notch (ductile crack region) reduces. This was demonstrated with ordinary tensile testers, which can give times-to-break down to about 1 s. But a more dramatic change occurs at higher speeds, such as can be imposed by a falling pendulum, with breaks in a fraction of a second, or even faster with ballistic impact. The typical form is a mushroom end, shown for nylon in **6A(1)**. The detail of the broken end in **6A(2)** shows a smooth, partly globular appearance which suggests melting of the material.

The reason for the difference from slow breaks is a change from isothermal to adiabatic conditions. At low speeds heat can be lost to the surroundings, but at high speeds the heat of drawing warms up the fibre in the region of the break. The softening, near melting, presumably then allows break to occur by localized flow of viscous material, so that any initial crack geometry is lost, and the snap-back after break causes the material to collapse into the mushroom cap. The exact shape of the end will depend on details of the thermomechanical forces.

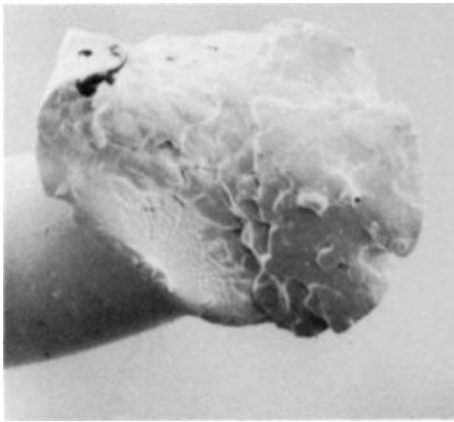
Sometimes, as in **6A(3)**, there is evidence of initiation at the surface and a vestigial V-notch region. In other circumstances there is a more distinct small V-notch, and this is usually so when the break is a little slower, as in **6A(4)**. It is interesting to note that there are two stages in the crack propagation, and the final rupture shows more globular indications of melting or softening. At higher speeds, as in **6A(5)**, the mushroom head may be smaller. Similar mushroom cap breaks are found in polyester fibres broken at high speed **6A(6)**. This picture also shows transverse striations along the length of the fibre which may be due to snap-back effects.



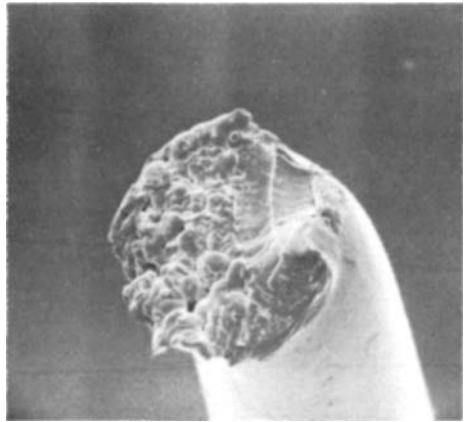
1

|—| 10  $\mu\text{m}$ 

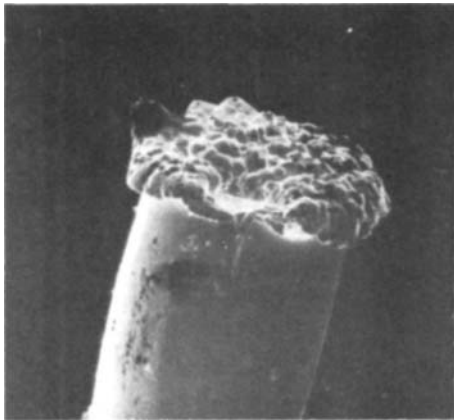
2

|—| 10  $\mu\text{m}$ 

3

|—| 10  $\mu\text{m}$ 

4

|—| 10  $\mu\text{m}$ 

5

|—| 10  $\mu\text{m}$ 

6

|—| 5  $\mu\text{m}$ 

**Plate 6A Nylon 66 fibres, 17dtex.**

(1) Broken by a pendulum falling from a 90° angle. (2) Broken, as in (1), showing detail of end. (3) Broken, as in (1), showing a small V-notch. (4) Broken by a pendulum falling from a 45° angle. (5) Broken by a relaxation catapult:

**Polyester.**

(6) Pendulum break showing mushroom head and transverse striations.

# 7

## AXIAL SPLITS

### Para-aramid (Kevlar), high-modulus polyethylene (HMPE), nylon at low temperatures

Highly oriented, highly crystalline, linear polymer fibres, such as the para-aramid Kevlar, show very high strength (more than 2 N/tex or 3 GPa) and an almost linear stress-strain curve like line (a) in Fig. 3.2. They break through the development of long axial splits in the filaments, 7A(1),(2).

If the fibre was perfectly uniform and subject to pure tension, there would be no stress across planes parallel to the fibre axis, and so no reason for axial splitting. But if there is any discontinuity or defect, either on the surface of the fibre or internally, this will give rise to a shear stress as shown in Fig. 7.1. (a). As the load on the fibre is increased, the shear stress rises, eventually overcoming the transverse cohesive forces and causing an axial crack to form, Fig. 7.1(b). If the crack is slightly off axis, it will eventually cross the fibre and lead to rupture, Fig. 7.1(c). Failure occurs in this way because even a small shear stress will overcome the weak intermolecular bonds between the polymer molecules before the large tensile stress breaks the covalent bonds within the chain molecules, as indicated schematically in Fig. 7.2. The difference may be accentuated by structural discontinuities.

In a majority of tensile breaks, it has been found that one end shows multiple splits, 7A(1), whereas the other end shows a single split, 7A(2). This is not due to any asymmetry in the material or the test method, but is a consequence of geometry. In Fig. 7.3(a), a split develops from a surface flaw, and then divides by bifurcation to give multiple cracks. However, if all the cracks develop at the same rate, the one on the outside must reach the other edge of the fibre first, giving the one end with a single split, and the other with multiple splits, as in Fig. 7.3(b). Even if one of the inner cracks develops faster, it would not give a simple pattern of multiple splits on each end, but would be a more complicated form, with re-entrant cracks on one end, as shown in Fig. 7.3(c).

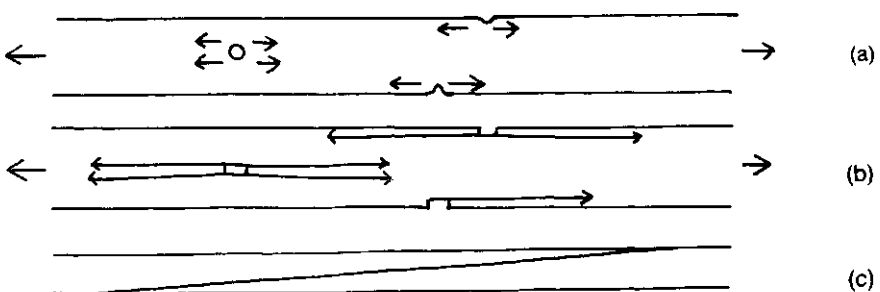


Fig. 7.1 — (a) Shear stresses at discontinuities in a fibre under tensile stress. (b) Shear stresses causing single or multiple cracks. (c) Crack at an angle to fibre axis, running across fibre and forming a break.

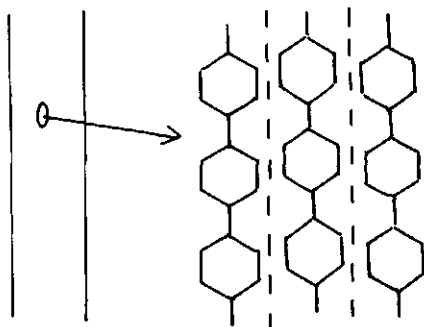


Fig. 7.2 — Schematic illustration of strong covalent bonds parallel to fibre axis contrasted to weak intermolecular bonds.

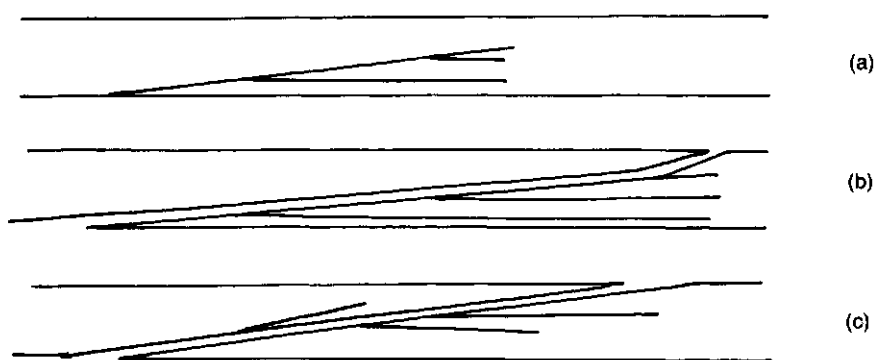


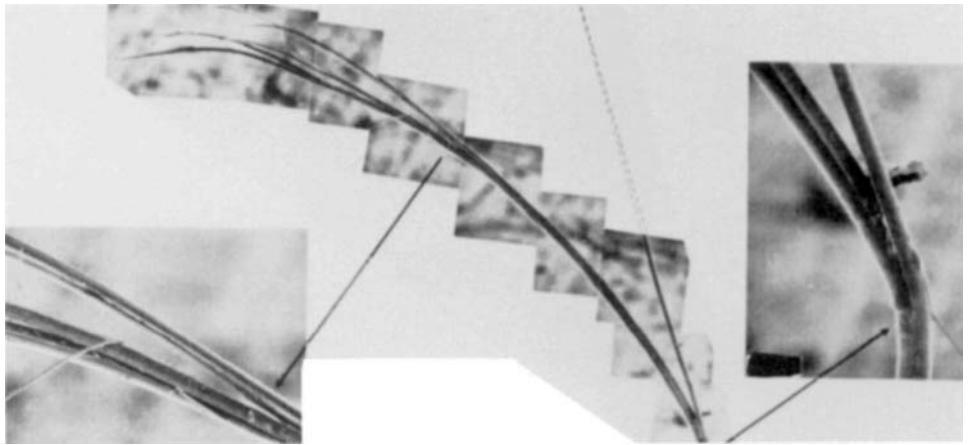
Fig. 7.3 —(a) Split propagated from one side of fibre with bifurcation, with all cracks propagating at the same rate. (b) When split reaches other side, one end of the break is a single split and the other has multiple splits. (c) If one of the inner cracks were to grow faster, a different pattern of splits would be observed in the broken fibres.

Fracture of Kevlar in liquid nitrogen, **7A(3)**, shows a similar long axial split, but interesting transverse striations can be seen along the split surfaces. Another example of the pronounced axial splitting is shown in **7B(1),(2)**.

The release of elastic energy, following rupture, can cause other features to appear. Snap-back along unbroken fibre leads to intense kinkband formation, **7B(3)**, due to an internal buckling of the oriented structure. Fibrillated portions may buckle as a whole into helices, **7B(4)**, and more complicated local splitting and buckling may occur, **7B(5),(6)**.

High-modulus polyethylene is another fibre which breaks with axial splitting, **7C(1)–(4)**. This is to be expected, because it is also a very highly crystalline and highly oriented fibre with high strength.

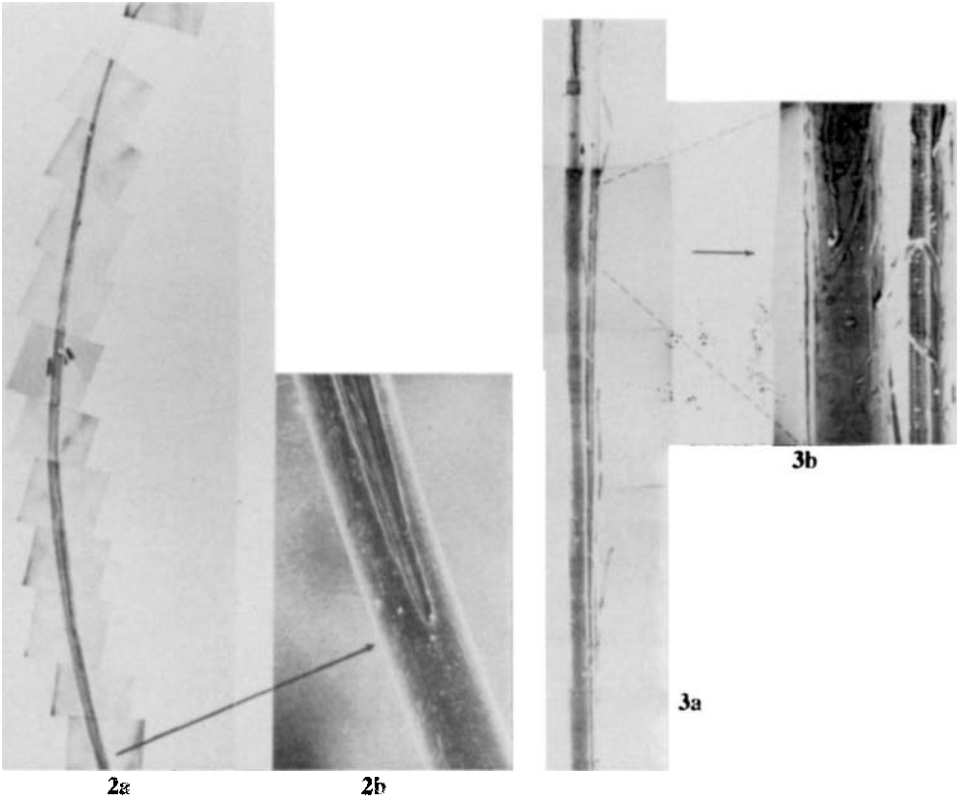
Ordinary nylon fibres broken at low temperatures, by means of immersion in liquid nitrogen while being extended on an Instron tester, also often show breakage by long axial splitting, **7C(5),(6)**. However, long splits were not obtained when special precautions were taken to ensure that the jaws and the test fibre were strictly aligned and there was no twist in the fibre. The splitting thus appears to be caused by the presence of small shear stresses, in addition to the larger tensile stress. At such low temperatures, internal chain mobility through rotation round bonds will be blocked and the material will be glassy. Ductile behaviour changes to brittle, with the load–elongation curve ending sharply without yield, so that a different form of break would be expected. However, it is surprising that it is so easy to cause transverse cohesion to give way before the axial cohesion, even at a moderate degree of orientation.



1b

1a

1c



2a

2b

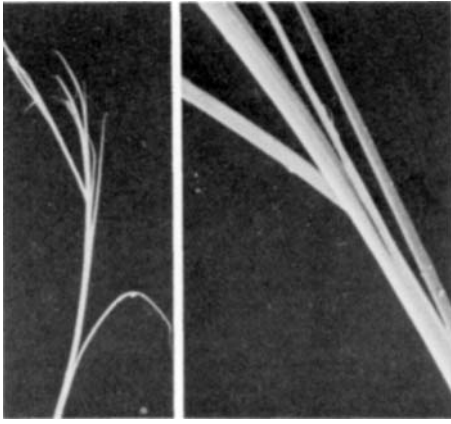
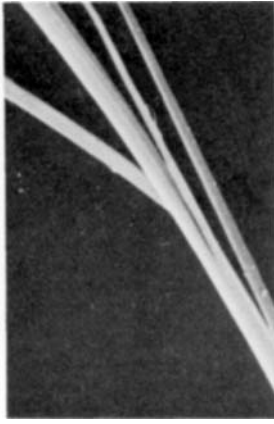
3b

3a

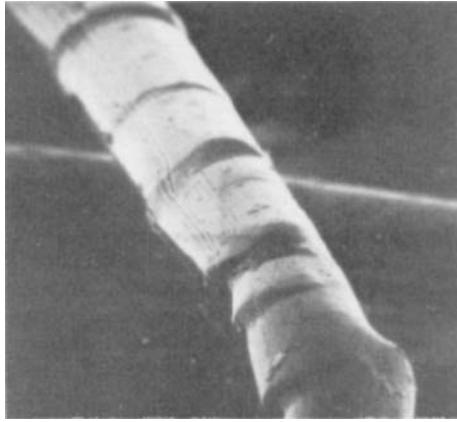
**PLATE 7A — Tensile breaks of aramid (Kevlar 29) fibres.**

(1a,b,c),(2a,b) Opposite ends of break, one showing multiple splitting and one showing a single split.

(3a,b) Fracture in liquid nitrogen.

1a | 100  $\mu\text{m}$ 1b | 20  $\mu\text{m}$ 

2

| 20  $\mu\text{m}$ 

3

| 50  $\mu\text{m}$ 

4

| 20  $\mu\text{m}$ 

5

| 50  $\mu\text{m}$ 

6

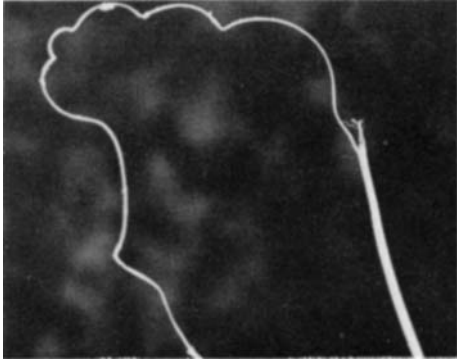
| 5  $\mu\text{m}$ 

**Plate 7B — Tensile breaks of aramid (Kevlar 29) (continued).**

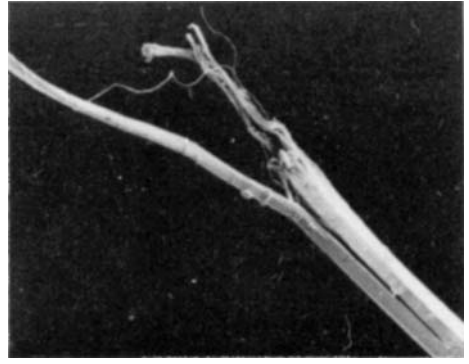
(1a,b),(2) Break with two details at higher magnification.

**Snap-back effects in Kevlar 49.**

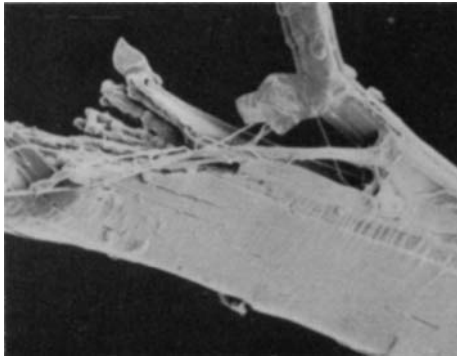
(3) Kink-bands along fibre. (4) Helical deformation of ribbon-like fibril. (5),(6) Complicated coiling, with detail of splitting.



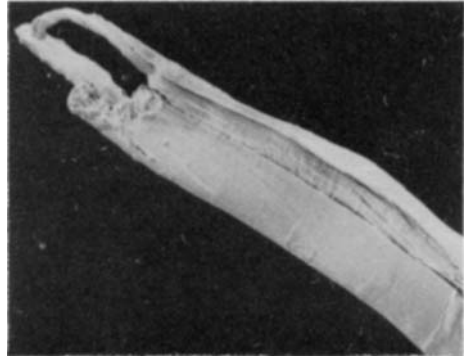
1

500  $\mu\text{m}$ 

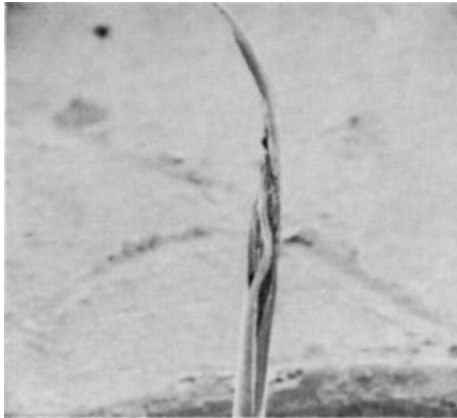
2

50  $\mu\text{m}$ 

3

20  $\mu\text{m}$ 

4

20  $\mu\text{m}$ 

5

100  $\mu\text{m}$ 

6

10  $\mu\text{m}$ 

**Plate 7C — Tensile breaks of high-modulus polyethylene (Allied Spectra 900) fibres.**

(1)–(3) Breaks of one end at increasing magnification. (4) Break of other end.  
Tensile break of nylon 66 in liquid nitrogen.

(5),(6) Break, shown at two magnifications.

# 8

## GRANULAR FRACTURE Solution-spun fibres

A group of poorly crystalline fibres, mostly with rather strongly interactive molecules, and all spun from solution, have stress-strain curves like line (d) in Fig. 3.2, showing an initial elastic region which yields at about 2% extension to an easily extensible region of poor recovery. Such fibres include viscose rayon (cellulose), acetate (cellulose diacetate and triacetate) and acrylic (polyacrylonitrile). They break to give a granular surface running more or less perpendicularly across the fibre, **8A(1)**. Similar breaks occur in cotton and wool fibres in some circumstances (see Chapters 18 and 19), and in alumina and carbon fibres, as mentioned at the end of this chapter.

In rayon, **8A(1)–(3)**, and even more in acetate fibres, **8A(4)–(6)**, there are many cracks visible all along the fibre. This means that the whole fibre is everywhere on the verge of failing when one section breaks. Indeed, it has been known for a triacetate fibre to be lost on rupture because it shattered into a cloud of tiny pieces. An incipient form of this sort of break-up is shown in **8A(5)**, where at a point remote from the actual break an acetate fibre has almost broken into two.

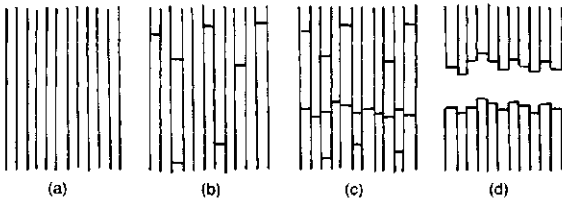
Triacetate fibres, **8A(6)**, break in a similar way, but the fracture surface is smoother. The sharpness of the granulation decreases from cellulose (viscose rayon) to secondary cellulose acetate to cellulose triacetate. This change is associated with ease of melting, which determines the effect of the heat generated during plastic deformation on the surface appearance. Cellulose, which is strongly hydrogen-bonded, will not melt, but at a high temperature it chars; secondary acetate melts with some difficulty; but triacetate is truly thermoplastic so that softening due to heat leads to the smoother, rounded surface of the break.

Granular breaks look very like a low-magnification view of the break of an oriented fibre composite, but, for such a material, the magnification can be increased, and the grains are resolved into individual fibre breaks separated by matrix. At a much finer level of structure, similar discontinuities must exist within fibres showing granular breaks. It has, in fact, been shown by Knudsen (1963) that during their spinning acrylic fibres coagulate from solution to give a spongy structure with excess solvent filling voids in the fibre. In the subsequent stretching and drying, the voids elongate, collapse and apparently disappear. But it is likely that the original void surfaces remain as weak boundaries separating the material into separate fibrillar elements.

Fig. 8.1(a) shows an idealized view of such a structure. When the tension reaches a certain level, elements will begin to break, Fig. 8.1(b), but the discontinuity prevents the occurrence of a large enough stress concentration to cause the crack to continue propagating across the fibre. However, there is some cohesion between elements, and excess stress is transferred to neighbouring elements which are thus more likely to break at a nearby position. Eventually the failure becomes cumulative over a cross-section, Fig. 8.1(c), and the granular break results, Fig. 8.1(d). The granular surface is clearly shown in the Courtelles acrylic (PAN) break, **8B(1),(2)**.

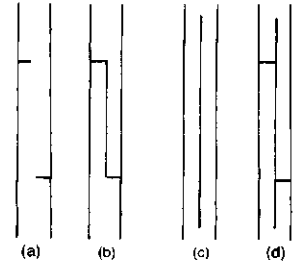
There can be deviations from the simple granular form. Sometimes, although the detail on the surface is granular, the overall effect shows evidence of ductile crack propagation, which was shown in its simplest form in Chapter 5, with a V-notch leading to catastrophic failure. This is just detectable in the Courtelles break, **8B(1),(2)**, and is very clear in the Acrilan carpet fibre, **8B(3)**. An incipient development of such a crack is shown in **8B(4)**.

In other fibres the break occurs at two places, linked by an axial split, to give a stepped break. There is a slight indication of this in the viscose rayon fibre, **8A(2)**, but the steps are very distinct in the acrylic fibres, **8B(5),(6)**. The separation between the steps can be many fibre



8.1

Fig. 8.1 — (a) Structure of separate elements. (b) Under tension, elements start to break. (c) Stress transfer causes cumulative break over a cross-section. (d) Granular breaks.



8.2

Fig. 8.2 — Mechanism of formation of stepped break. Alternative 1: (a) two breaks form; (b) breaks join up by axial split. Alternative 2: (c) fibre containing axial split; (d) two parts break independently.

diameters, **8B(6a)**. It is not clear whether two breaks form and then join up by the axial split, as in Fig. 8.2(a,b), or whether the fibre is already split axially into two parts, which then break independently, as in Fig. 8.2(c,d).

In one special case, **8A(3)**, the break occurred preferentially at a weak place in the fibre caused by the presence of large voids, which reduced the area of material available to carry load.

Bicomponent acrylic fibres may break without showing any very special features, **8C(1)**, but they may also show splitting between the two components, **8C(2)–(6)**, with granular breaks and continuing splits at several different places in the fibre.

Other solution-spun organic fibres which show similar forms of break are polyvinyl alcohol (PVA), **8D(1),(2)**, where the 'granules' on the surface become elongated projections, and the advanced engineering thermally resistant fibre, polybenzimidazole (PBI), **8D(3)**.

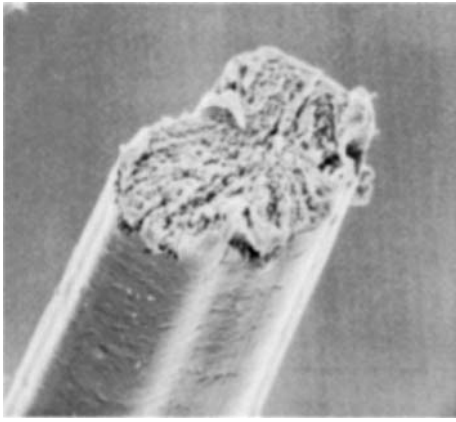
Granular breaks are also found in some high-modulus fibres, such as the alumina fibre, DU PONT FP3, **8D(4)**. This fibre is made by extruding an aqueous slurry of alumina and spinning additives, drying, and then heating the fibre to a high temperature. Evidently, the method of manufacture leads to a granular structure which shows up in the break. The influence of the mode of formation is clearly shown in breaks of carbon fibres, **8D(5),(6)**, which have features similar to those of the precursor PAN or PVA fibres. Other forms of alumina and carbon fibre, illustrated in Chapter 4, show different break appearances.

As stated in the first paragraph of this chapter, fibres spun from solution typically show granular breaks, such as those in **8A(1)–(3)** for cellulose fibres produced by the viscose process. Tensile breaks of Tencel, show similar granular fractures; this is a *lyotropic* fibre from Courtaulds, made by a new process for regenerating fibres directly from a solution of cellulose in an organic solvent. The break can be seen to fan out from an incipient initial crack in **8E(1),(2)** and more prominently in **8E(3)**. In **8E(4),(5)**, the break divides into steps, and in **8E(6)** splits to a greater extent.

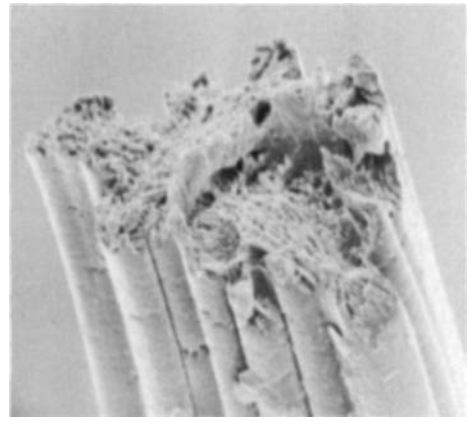
**8F(1),(2)** shows granular fractures similar to **8A(2)** and **8D(5)**, in acrylic (PAN) fibres after initial thermal stabilisation. **8F(3)–(6)** shows granular fractures in melt-spun polyester fibres loaded with barium sulphate.

Granular breaks of carbon fibres were shown in **8D(5),(6)**. A recent investigation by Boyes and Lavin of DU PONT has demonstrated how the use of a high resolution SEM, referred to in Chapter 1, can be used to show up differences in the fracture of carbon fibres from different precursors. **8G(1)–(3)** are for high modulus PAN-based carbon fibres. **8G(1)** shows a clean break with a nubby surface texture. **8G(2)** shows a skin-core effect and a braided texture, which may result from aggregations of polymer chains. At the highest magnification, the cross-section in **8G(3)** demonstrates the very small scale of the texture. In contrast to this, the cross-section of a high modulus pitch-based carbon fibre in **8G(4)** shows many long crystal planes parallel to the yarn axis, following zig-zag paths across the fibre. This influences the composite character of the granular break of the pitch-based fibre, as shown in **8G(5)**. At a higher magnification, **8G(6)**, the length and perfection of the carbon crystal planes becomes apparent.

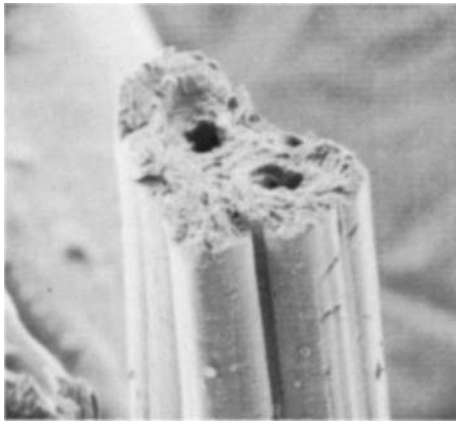
The SEM pictures of ceramic fibres in **8H** were obtained by Bunsell and colleagues at Ecole des Mines de Paris.



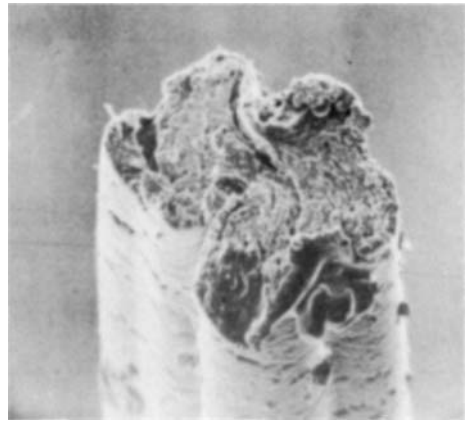
1

5  $\mu\text{m}$ 

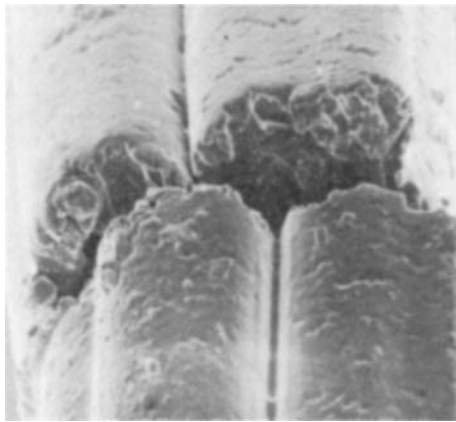
2

5  $\mu\text{m}$ 

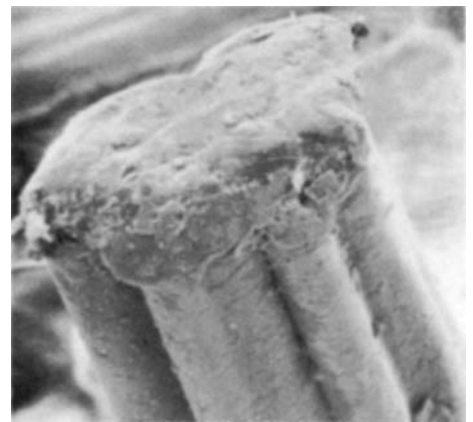
3

10  $\mu\text{m}$ 

4

5  $\mu\text{m}$ 

5

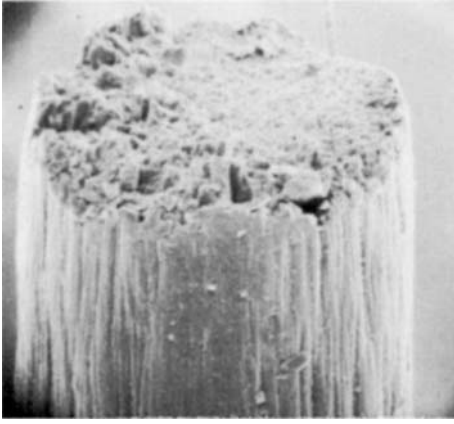
2  $\mu\text{m}$ 

6

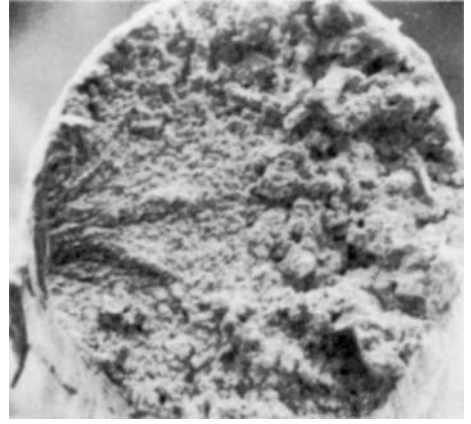
10  $\mu\text{m}$ 

**Plate 8A — Tensile breaks of cellulosic fibres.**

(1) 3.3 dtex polynosic viscose fibre (Vincel). (2) 14.7 dtex viscose rayon fibre. (3) 20 dtex viscose rayon fibre with holes at point of break. (4) 4 dtex secondary acetate fibre (Dicel). (5) Cracks on surface of broken acetate fibre, near to breakage. (6) Triacetate fibre (Tricel).



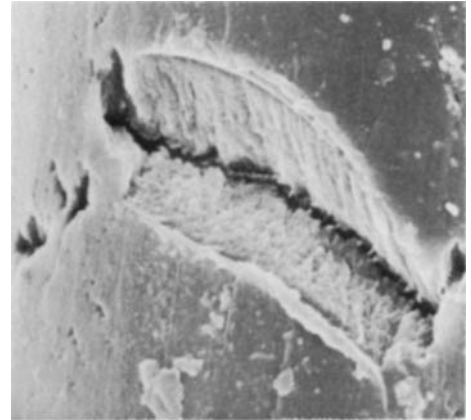
1

5  $\mu\text{m}$ 

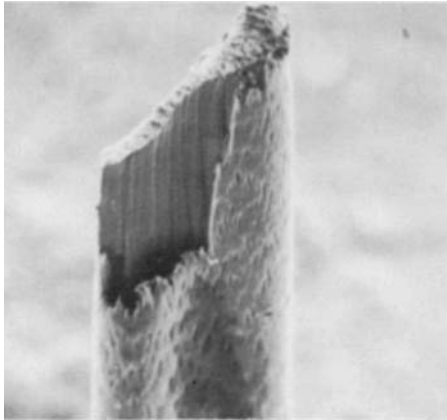
2

5  $\mu\text{m}$ 

3

10  $\mu\text{m}$ 

4

2  $\mu\text{m}$ 

5

10  $\mu\text{m}$ 

6a

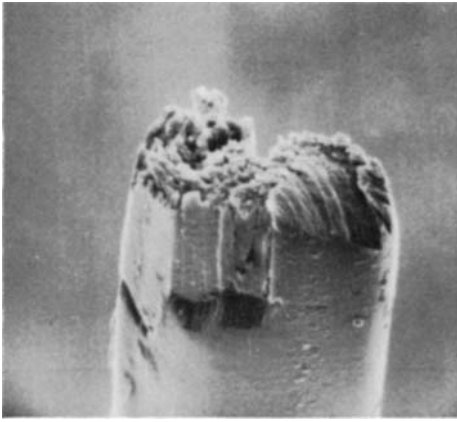
50  $\mu\text{m}$ 

6b

5  $\mu\text{m}$ 

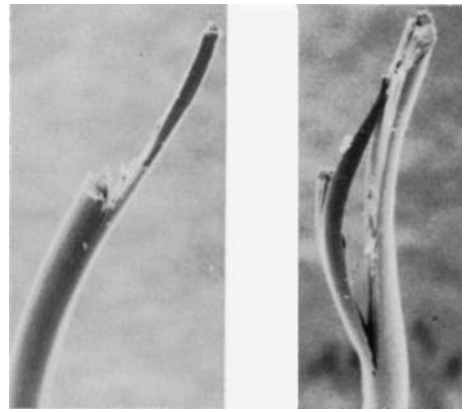
**Plate — 8B — Tensile breaks of acrylic fibres.**

(1),(2) 16.7 dtex Courttelle; two views of same break. (3) 16.7 dtex Acrilan. (4) Crack development in Acrilan, at a position away from the break. (5) 7 dtex Orlon 42. (6a,6b) 3.3 dtex Courttelle.



1

|—| 10 μm



2a

|—| 50 μm

2b

|—| 50 μm



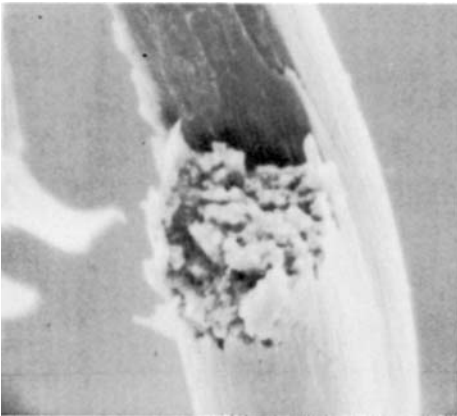
3

|—| 20 μm



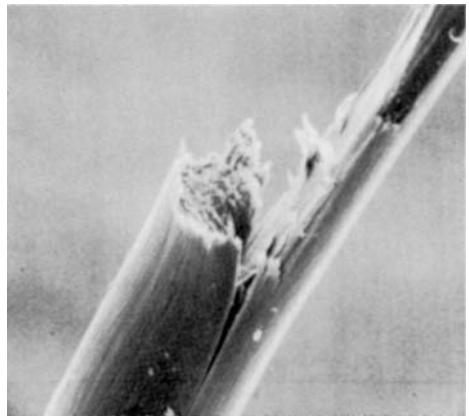
4

|—| 10 μm



5

|—| 5 μm

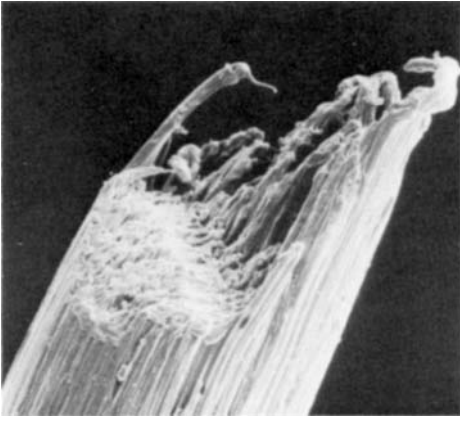


6

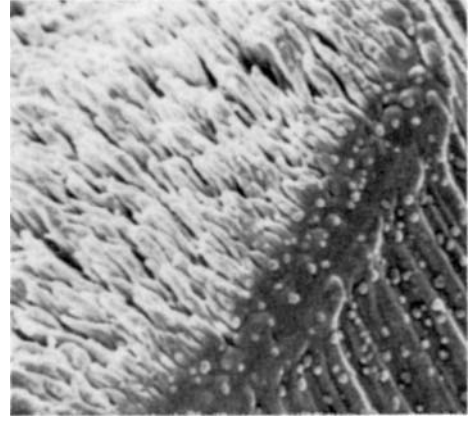
|—| 20 μm

**Plate 8C — Tensile breaks of 18 dtex bicomponent Acrilan acrylic fibre.**

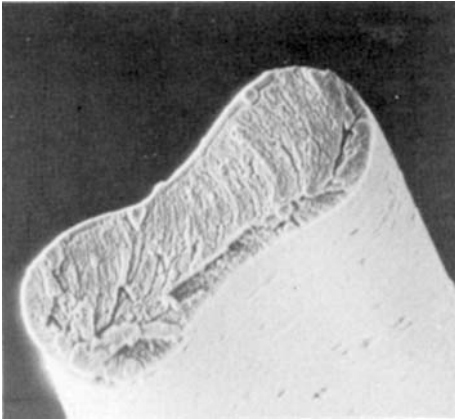
(1) Relatively simple break, with some evidence of initial crack formation, and a small step at the edge. (2a,b) Opposite ends of another break. (3) Enlarged view of end (2a). (4) Tip of end (2b), which fits into step on (2a), shown in (3). (5) Detail of step break on middle of lower part of (2b). (6) Continuing split at step on end (2a).



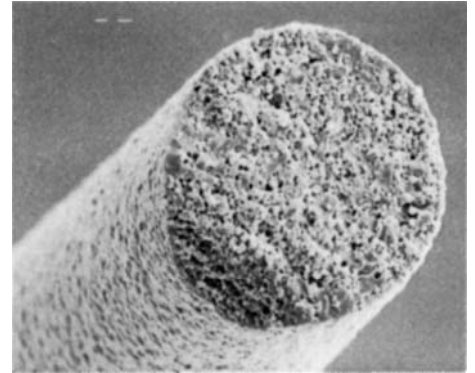
1

5  $\mu\text{m}$ 

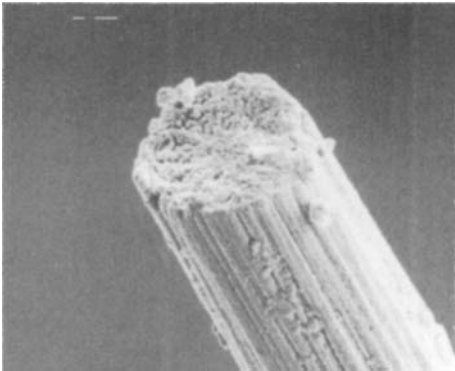
2

2  $\mu\text{m}$ 

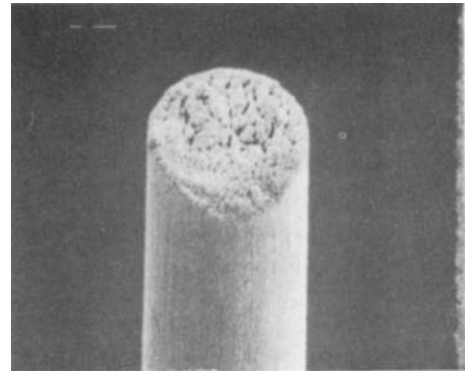
3

2  $\mu\text{m}$ 

4

5  $\mu\text{m}$ 

5

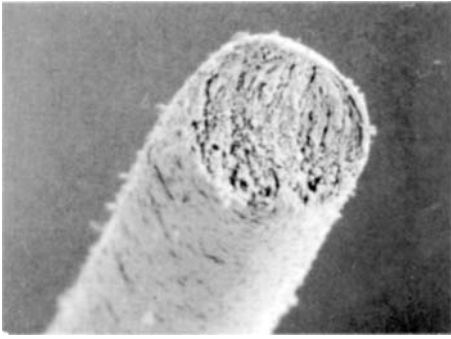
5  $\mu\text{m}$ 

6

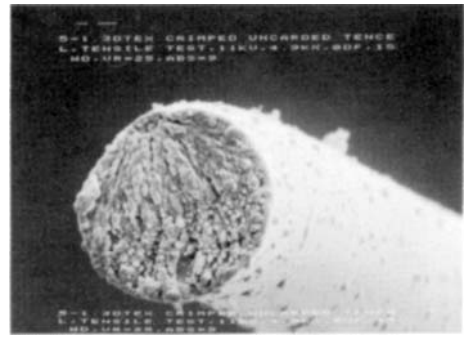
5  $\mu\text{m}$ 

**Plate 8D — Tensile breaks of other fibres.**

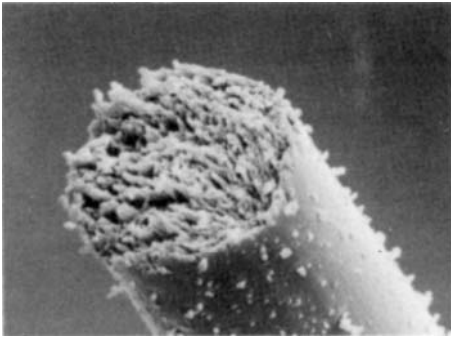
(1),(2) Polyvinyl alcohol fibre (PVA). (3) Polybenzimidazole fibre (Celanese PBI). (4) Alumina fibre (DU PONT FP3). (5) Carbon fibre, PAN precursor. (6) Carbon fibre, PVA precursor.



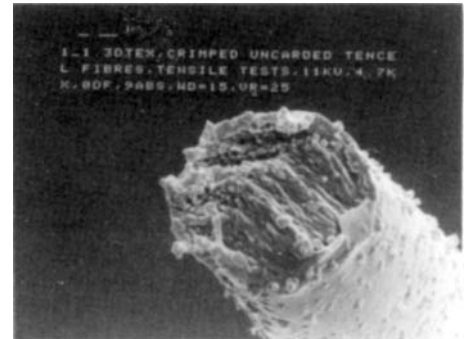
1



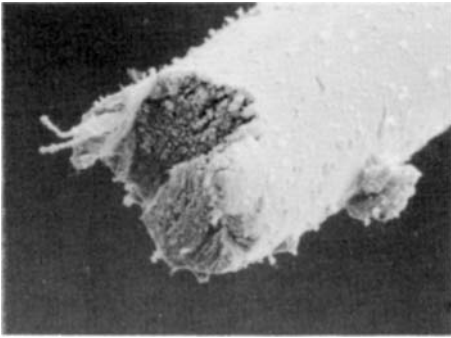
2



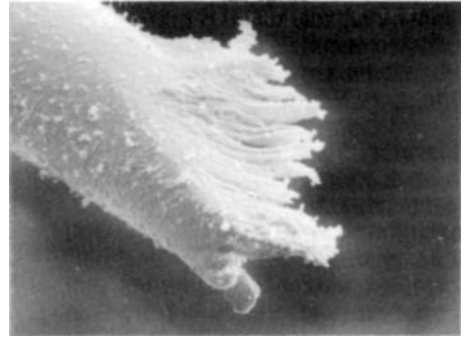
3



4



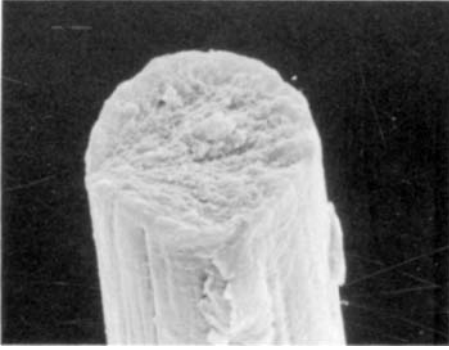
5



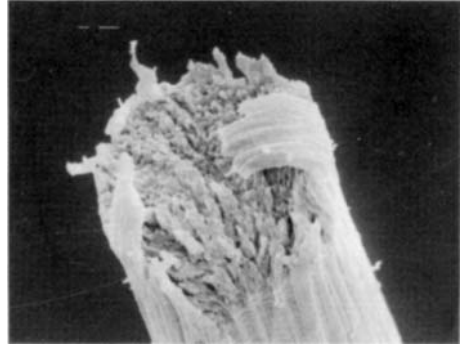
6

Plate 8E — Tensile breaks of *Tencel* fibres.

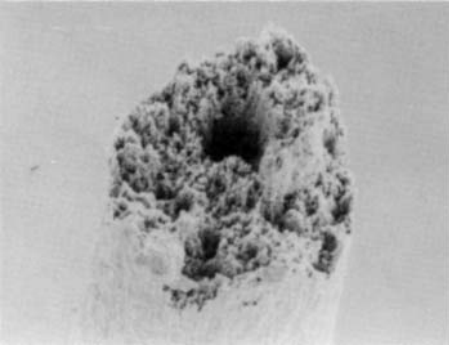
(1)-(6) Granular breaks of varying complexity.



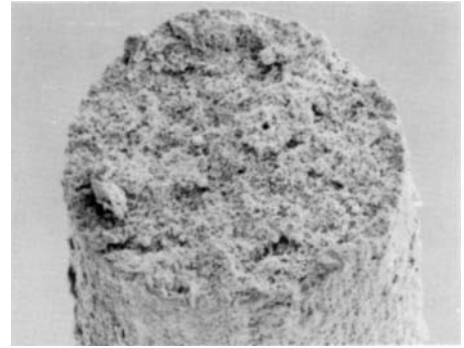
1



2



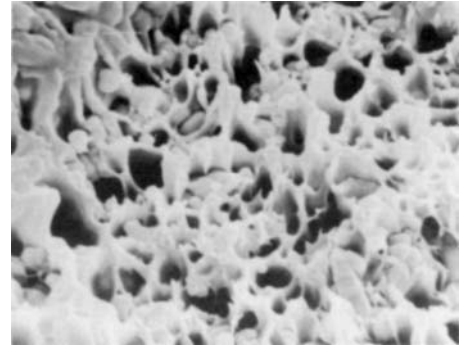
3



4



5



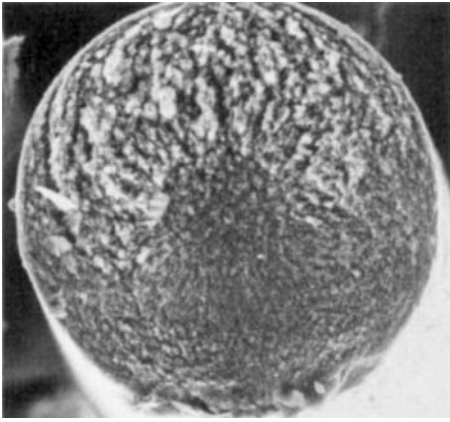
6

**Plate 8F — Tensile breaks of oxidized PAN fibres.**

(1) Fibre stabilized for 90 minutes at 250°C. (2) Stabilized for 15 minutes.

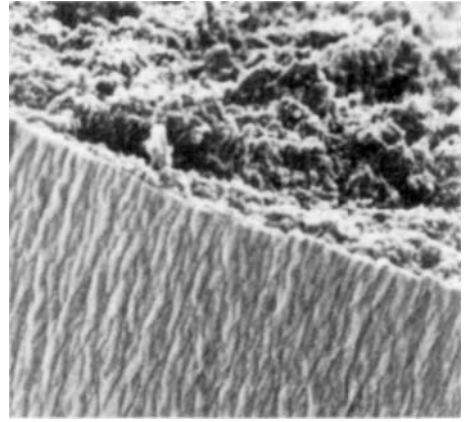
**Tensile breaks of polyester fibres loaded with barium sulphate.**

(3) Fibre with 60% barium sulphate. (4)–(6) Fibres with 70% barium sulphate at different magnifications.



1

|&lt;— 3 µm —&gt;|



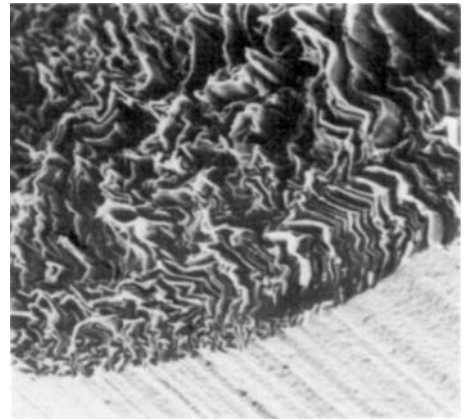
2

|&lt;— 1.5 µm —&gt;|



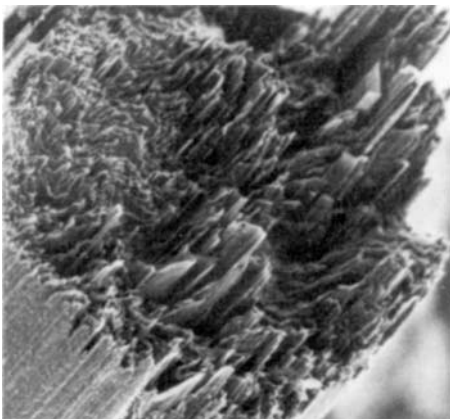
3

|&lt;— 300 nm —&gt;|



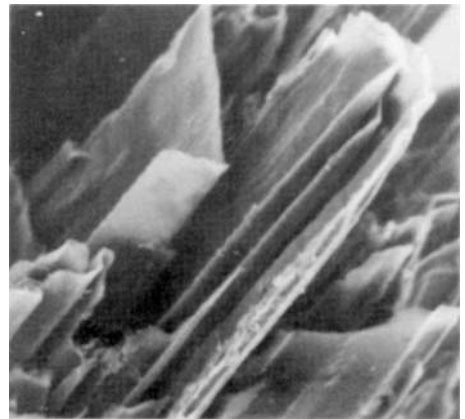
4

|&lt;— 1.2 µm —&gt;|



5

|&lt;— 3.0 µm —&gt;|

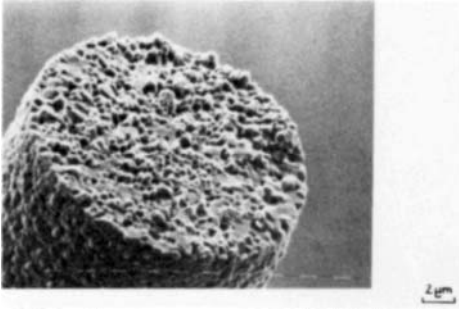


6

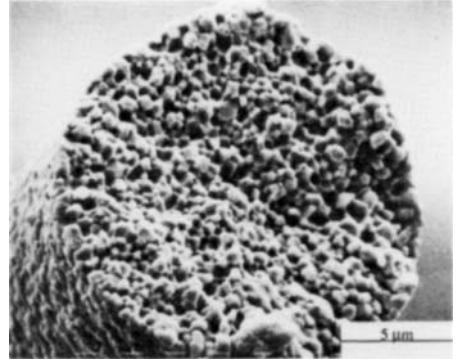
|&lt;— 0.7 µm —&gt;|

**Plate 8G — Carbon fibres viewed in high-resolution SEM, by courtesy of E.D. Boyes and J.G. Lavin, Central R&D, DuPont Co.**

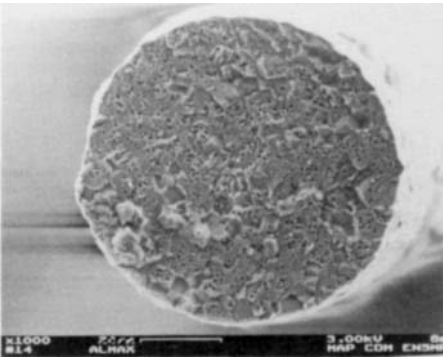
(1),(2) Tensile breaks of high modulus PAN-based carbon fibres. (3) Cross-section of PAN-based fibre at high magnification. (4) Cross-section of high modulus pitch-based carbon fibre. (5),(6) Tensile breaks of pitch-based fibres.



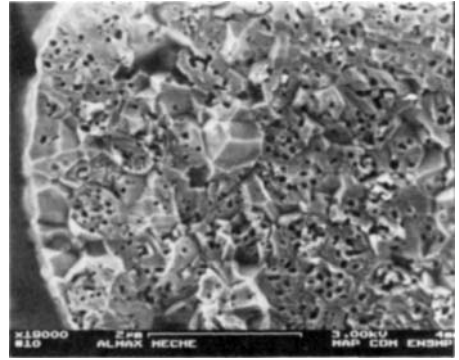
1



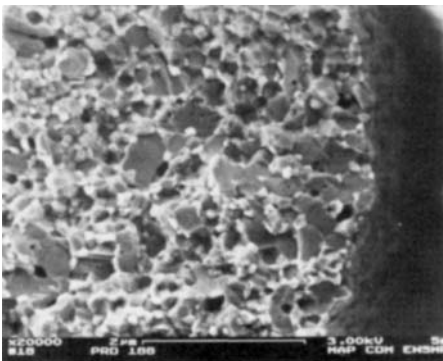
2



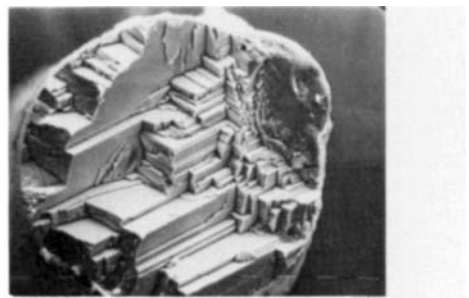
3



4



5



6

**Plate 8H — Breaks of ceramic fibres, by courtesy of A.R. Bunsell, Centre des Materiaux de l'Ecole des Mines de Paris.**

(1) Tensile break of FP alumina fibre at room temperature. (2) Creep failure of FP fibre at 1300°C. (3), (4) Break of Almax alumina fibre. (5) Break of PRD 166, alumina with zirconia, fibre. (6) Break of single crystal Saphikon  $\alpha$ -alumina fibre.

# 9

## FIBRILLAR FAILURE Wet cotton

Cotton breaks in tension in different ways, depending on the humidity and the chemical treatments applied to the fibre. This diversity is explored in Chapter 18. However, one form of break is introduced here, because it is a distinct identifiable mode of separate fibrillar failure, 9A(1)–(4).

Cotton is known to be an assembly of crystalline microfibrils, and when wet the fibrils will be separated by layers of absorbed water molecules. The interaction between the fibrils will be very weak, and they break independently, as indicated in Fig. 9.1(b). When all the fibrils have broken, Fig. 9.1(c), the two ends separate, Fig. 9.1(d): the fibre has broken. The ends of the break will be a collection of fibrils, or groups of fibrils, which may collapse into a tapered end under the surface tension of the water as the fibre dries, Fig. 9.1(e). These features can be seen in 9A(1)–(4).

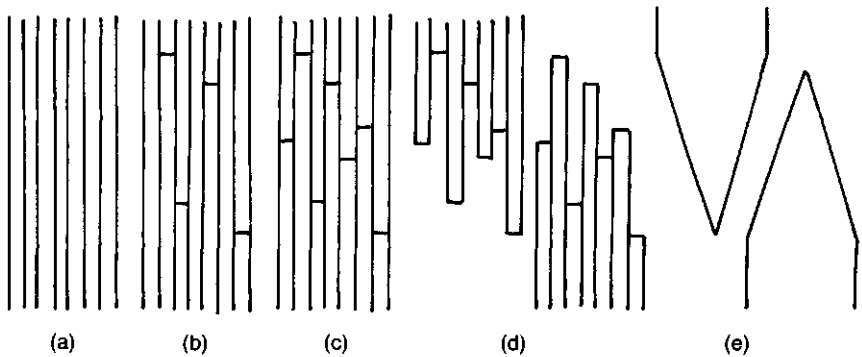
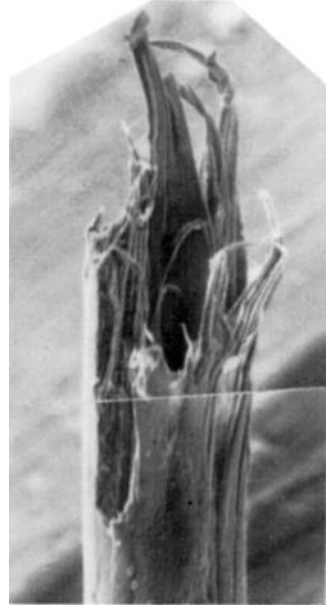


Fig. 9.1 — Schematic representation of independent fibrillar break. (a) Structure of separate fibrils, only weakly linked. (b) Under sufficient tension, fibrils begin to break. (c) Finally all fibrils have broken and the ends can separate. (d) Two broken ends. (e) Possible collapse to tapering ends.



1

|—| 10  $\mu\text{m}$ 

2

|—| 5  $\mu\text{m}$ 

3

|—| 10  $\mu\text{m}$ 

4

|—| 5  $\mu\text{m}$ 

**Plate 9A — Tensile breaks of wet cotton.**

(1) Raw cotton. (2)–(4) Mercerized cotton.